Spatiotemporal regulation of circular RNA expression during the developmentof skeletal muscle, subcutaneous fat, and liver in Ningxiang pigs

Biao Li
Hunan Agricultural University
Yan Gong
Hunan Agricultural University
Yuebo Zhang
Hunan Agricultural University
Kyung Seok Kim
Iowa State University
Yu Xiao
Hunan Agricultural University
Qinghua Zeng
Hunan Agricultural University
Kang Xu
Chinese Academy of Sciences
Yehui Duan
Chinese Academy of Sciences
Jianhua He
Hunan Agricultural University
Haiming Ma (mahaiming2000@163.com)
Hunan Agricultural University https://orcid.org/0000-0002-2702-2440
Jun He
Hunan Agricultural University

Research article

Keywords: circRNAs, Ningxiang pig, profiling, skeletal muscle, liver, subcutaneous fat

Posted Date: December 11th, 2020

DOI: https://doi.org/10.21203/rs.3.rs-124585/v1

Abstract

Background

In recent years, thousands of different circular RNAs (circRNAs) have been identified through comparative analysis of different pig breeds. However, very few studies have investigated the spatiotemporal expression patterns of circRNA during organ development, which is crucial for functional and evolutionary analysis.

Results

In this study, we systematically analyzed circRNAs associated with fatty acid metabolism in the three main organs (muscle, fat and liver) a tfour growth time points (30 d, 90 d, 150 d and 210 d after birth) for Ningxiang pigs, awell-known native pig breed in China known for its excellent meat quality. We identified 61,683 circRNAs and analyzed their molecular characteristics, potential functions, and interactions with miRNAs. The circRNAs exhibited notable spatiotemporal specificity in the form of dynamic expression. At 90 d, the number and complexity of differentially expressed circRNAs in the liver was the highest.We used STEM (Short Time-series Expression Miner) to perform time series analysis on differentially expressed circRNAs and observed that there were multiple model spectra that were significantly enriched with time changes in all three organs. All the significantly changed circRNAs, miRNAs and mRNAs obtained from STEM analysis of each tissue were utilized to confirm that the circRNA and mRNA have a targeting relationship with miRNA. Notably, we screened 2384 (fat), 2672 (muscle) and 9187 (liver) circRNA-miRNA-mRNA network pairs related to developmental time changes. Finally, we used fluorescence *in situ* hybridization (FISH) to demonstrate the dynamic subcellular localization of circRNA during development.

Conclusion

These data suggest that circRNA is highly abundant in muscle, fat and liver and is dynamically expressed in a spatiotemporal manner. These results suggest that circRNAs play important roles in fat metabolism in Ningxiang pigs. Our findings also provide new ideas and perspectives for the study of Ningxiang pigs' lipid metabolism regulation pathway and meat quality traits.

Background

After years of breeding work, the lean meat rate of pigs has been considerably improved, but the improvement of living standards has also prompted consumers to seek pork with higher meat quality. Chinese indigenous breeds are known for their quality meat production, and there have been some reports of using Chinese native pigs as a biological model to study meat quality traits[1]. Ningxiang pigs are well-known for their excellent meat quality and have become one of the four best-known local breeds in China. It has been reported that unsaturated fatty acids (UFAs) in Ningxiang pork account for up to 59.6% of all fatty acids[2].Moreover, He etal.[3] found that the serum of Ningxiang pigs contains more unsaturated lipids than that of lean pigs under the same environment and feeding conditions. Polyunsaturated fatty acids (PUFAs) are indispensable essential fatty acids for the body, while long-chain (≥ C20) polyunsaturated fatty acids (LC-PUFAs) are highly biologically active forms of PUFAs, and their biological functions have become a heavily researched topic in international research[4, 5].This characteristic is a valuable trait of Ningxiang pig. It has been reported that the synthesis of unsaturated lipids is regulated by multiple genes, such as peroxisome proliferator activated receptor alpha (*PPARα*), fatty acid binding protein 4 (*FABP 4*), lipoprotein lipase (*LPL*)[6], CCAAT enhancer binding protein alpha (*C/EBPα*)[7], patatin-like phospholipase domain containing 3 (*PNPLA3*)[8], malic enzyme 1 (*ME1*)[9] and 2,4-dienoyl-CoA reductase 1 (*DECR1*)[10].Therefore, as a research model, Ningxiang pigs are of considerable significance for studies exploring genes related to meat quality traits and their expression patterns.

With the development of high-throughput sequencing technology, it has been shown that biological processes are regulated not only by protein-encoding RNAs (mRNAs) but also by noncoding RNAs (ncRNAs), such as microRNAs (miRNAs) and circular RNAs (circRNAs). CircRNAs are a new group of noncoding RNAs characterized by the existence of circular structures in which the 3' ends are covalently bound to the 5' ends. Functional circRNAs have been demonstrated to function as cytoplasmic microRNA sponges and nuclear transcriptional regulators, indicating that these RNAs participate in the regulation of gene expression[11].There have been many reports indicating a large difference between fatty and lean pig breeds regarding the influence of circRNAs on pork quality.In a study of subcutaneous adipose tissue of Large White and Laiwu pigs, 275 differentially expressed circRNAs were identified, in which the target genes of circRNA_26852 and circRNA_11897 were found to be involved in adipocyte differentiation and lipid metabolism[12].The liver is a primary location for metabolic processes, such as lipid digestion, absorption, decomposition, synthesis and transportation. Adipose tissue is the primary energy storage organ and energy source of animals[13]. The amount of intramuscular fat (IMF) is related to the number of adipocytes and the ability to accumulate fat. Intramuscular fatty acids, especially polyunsaturated fatty acids, are important precursors of pork flavor substances that indirectly or directly affect indicators of meat quality, such as pH, water-holding capacity, tenderness, mouth feel, and meat color[14].However, the expression patterns and potential regulatory mechanisms of circRNAs related to meat quality or lipid anabolism in these organs across different developmental stages of pigs have rarely been reported.

In this study, we first compared circRNA expression levels among three major lipid metabolic organs/tissues of Ningxiang pigs, namely, longissimus dorsi muscle (muscle), subcutaneous fat (fat) and liver, atvarious developmental stages (30, 90, 150, and 240 d after birth). The molecular characteristics, spatiotemporal expression patterns, potential functions and targeted miRNAs of the organ samples were systematically analyzed. To explore the dynamic expression pattern of circRNAs, we adopted a time-series analysis by STEM and constructed a network diagram of circRNA-miRNA-mRNA interactions that significantly changed over time. Furthermore, screening circRNAs that affect fat metabolism throughout the developmental stages of pigs could significantly help to elucidate their biological and metabolic functions and relative importance.

Methods

Ethics Statement

The protocol for pig handling and treatment was in accordance with the recommendations of the Laboratory Animals Guideline of Welfare and Ethics of China. The study was approved by the “Institutional Animal Care and Use Committee of Hunan Agricultural University.”

Experimental Animals and Sample Collection

Twelve male purebred Ningxiang pigs were used in this study (all pigs were half-sibs). The experimental pigs were all provided by the Ningxiang pig breeding farm of Dalong Animal Husbandry Technology Co. Ltd. in Hunan Province, China. The 12pigswere examined at each of the four developmental stages in this study, including 30 d (30 d after birth), 90d(90 d after birth),150 d (150 d of age) and 210 d (210 d of age). Three biological repeats were employed per time point. The pigs were housed under standard environmental conditions (including unregulated room temperature and natural light) and fed three times per day on a standard diet with free access to water. Next, 3 healthy individuals with no disease and similar body weights were randomly selected in the 4 age groups from 30 d to 210 d in accordance with standard procedures. The pigs were fasted the following day. Next, the pigs were sacrificed by exsanguination under isoflurane anesthesia at the surgical plane (4.5% tidal volume by mask). The longissimus dorsi muscle, subcutaneous fat, and liver samples were collected within 30 min after the pigs were sacrificed, immediately frozen in liquid nitrogen and stored at -80 °C until analysis.

RNA Extraction

Total RNA was extracted from the tissue using Plant RNA Purification Reagent according the manufacturer’s instructions (Invitrogen), and genomic DNA was removed using rDNaseIRNase-free (TaKara). RNA quality was verified using a 2100 Bioanalyzer (Agilent Technologies,Santa Clara, CA, USA) and an ND-2000 spectrophotometer (NanoDrop Technologies). Only high-quality RNA samples (OD260/280 = 1.8 ~ 2.2, OD260/230 ≥ 2.0, RIN ≥ 6.5, 28S:18S ≥ 1.0, > 10 μg) were employed to construct a sequencing library.

Library Preparation and Illumina HiSeq X TenSequencing

The RNA-seq transcriptome strand library was prepared following the TruSeq^{TM}Stranded Total RNA kit from Illumina (San Diego, CA) using 5 μg of total RNA. Briefly, ribosomal RNA (rRNA) depletionin stead of poly(A) purification was performed using an IlluminaRibo-Zero Magnetic kit, first employing fragmentation by a fragmentation buffer. Second, first-stranded cDNA was synthesized with random hexamer primers. Next, we removed the RNA template and synthesized a replacement strand, incorporating dUTP in place of dTTP to generate ds cDNA. AMPure XP beads were utilized to separate the ds cDNA from the second-strand reaction mix. Asingle ‘A’ nucleotide was added to the 3’ ends of these blunt fragments to block them from ligating to one another during the adapter ligation reaction. Finally, multiple indexing adapters were ligated to the ends of the ds cDNA. Libraries were size-selected for cDNA target fragments of 200–300 bp on 2% Low Range Ultra Agarose followed by PCR amplification using Phusion DNA polymerase (NEB) for 15 PCR cycles. After quantification by TBS380, the paired-end RNA-sequencing library was sequenced with Illumina HiSeq X Ten(2 × 150-bp read length). In addition, 3 μg of total RNA was ligated with sequencing adapters with the TruSeq™ Small RNA Sample Prep Kit (Illumina, San Diego, CA, USA). Subsequently, cDNA was synthesized by reverse transcription and amplified with 12 PCR cycles to produce libraries. After quantification by TBS380, deep sequencing was performed by Shanghai Majorbio Bio-Pharm Biotechnology Co., Ltd. (Shanghai, China).

Read Mapping and Transcriptome Assembly

The raw paired-end reads were trimmed and quality-controlled by SeqPrep (https://github.com/OpenGene/fastp) with default parameters. Next, clean reads were separately aligned to the reference genome(accession number PPJNA531381) in orientation mode using HISAT2 (https://ccb.jhu.edu/software/hisat2/index.shtml) software. The mapped reads of each sample were assembled by StringTie (https://ccb.jhu.edu/software/stringtie/index.shtml) in a reference-based approach.

Identification of circRNAs

The CIRI2 (CircRNA Identifier 2) tool was used to identify circRNAs. This tool scans SAM files twice and collects sufficient information to identify and characterize circRNAs. Briefly, during the initial scanning of SAM alignment, CIRI 2 detects junction reads with PCC signals that reflect a circRNA candidate. Preliminary filtering is implemented using paired-end mapping (PEM) and GT-AG splicing signals for the junctions. After clustering junction reads and recording each circRNA candidate, CIRI 2scans the SAM alignment again to detect additional junction reads and performs further filtering to eliminate false positive candidates that may result from incorrectly mapped reads of homologous genes or repetitive sequences. Finally, identified circRNAs are output with annotation information. The expression level of each circRNA was calculated according to the spliced reads per billion mapping (SRPBM) method. Significantly differentially expressed(DE) circRNAs were extracted with $|\log2FC| > 1$ and P-values ≤ 0.05 by Deseq2.

Differential Expression Analysis and Functional Enrichment

To identify DEGs (differentially expressed genes) between two different samples, the expression level of each transcript was calculated according to the transcripts per kilobase of exon model per million mapped reads (TPM) method. RSEM (http://deweylab.biostat.wisc.edu/rsem/) was employed to quantify gene abundances. R statistical package software EdgeR (Empirical analysis of Digital Gene Expression in R,http://www.bioconductor.org/packages/2.12/bioc/html/edgeR.html) was utilized for differential expression analysis. In addition, functional enrichment analysis, including GO and KEGG analyses, was performed to identify which DEGs were significantly enriched in GO terms and metabolic pathways at P-values ≤ 0.05 compared with the whole-transcriptome background. GO functional enrichment and KEGG pathway analysis were performedusing Goatools (https://github.com/tanghaibao/Goatools)and KOBAS (http://kobas.cbi.pku.edu.cn/home.do).

Time-series Analysis

Time-series analysis was performed by STEM (Short Time-series Expression Miner)[15].Time-series analysis studies the dynamic behavior of gene expression and measures a series of processes that have strong correlations with time points. This analysis produces a color for backgrounds with significant profiles, while producing a white background for profiles that are not significant. Model profiles of the same color belong to the same cluster of profiles. Significantly enriched model profiles are indicated by different colors (Bonferroni-adjusted P-values ≤ 0.05). The corrected P-values are sorted from small to large.

Analysis of ceRNAs Regulatory Network

To reveal the role and interactions among ncRNAs and mRNAs, we constructed a ncRNA-mRNA regulatory network. MiRanda was used to predict the circRNA-miRNA-mRNA pairs (score cutoff ≥ 160 and energy cutoff ≤-20). The coexpression network of circRNA-miRNA-mRNA was constructed using Cytoscape software (v3.2.1) to investigate the function of key circRNAs[16].

RT-PCR

To validate the identified circRNAs in Ningxiang pigs, total RNA was extracted using an Animal Total RNA Kit (Tiangen, China) and treated with ribonuclease R (RNase R). cDNA was synthesized by reverse transcription using a RevertAid First Strand cDNA Synthesis Kit (Thermo Scientific, USA). The divergent PCR primers were designed using the “out-facing” strategy to exclude linear mRNA from amplification (synthesized by Sangon Biotech Co., Ltd., Shanghai, China). PCR products were validated by Sanger sequencing.

Fluorescence in situ**hybridization (FISH)**

Muscle samples fixed with 4% paraformaldehyde were cut sagittally into thick sections and dewaxed in paraffin sections in water. Next, the sections were boiled in repair solution for 10 min. Proteinase K (20 μg/mL) was added dropwise, allowed to react with the samples at 37 °C for 30 min, and washed away by rinsing with PBS for 5 min 3 times. Then, the prehybridization solution was added and incubated at 37 °C for 1 h. The Chr01_143206410_143210729 probe (5'-GCTTCCTGTTTTTTACTTGGGCTGTTAG-3') (General Biol, China) containing a hybridization solution was added at a concentration, and hybridization was performed at 37 °C overnight. The nuclei stained with DAPI (Servicebio, Wuhan, China) appeared blue under ultraviolet excitation, and positive expression was indicated by red fluorescence. The images were observed using an upright fluorescence microscope (Nikon, Tokyo, Japan).

Statistical analysis

Differential gene expression analysis based on the negative binomial distribution and used the DESeq2, which a method for differential analysis of count data, using shrinkage estimation for dispersions and fold changes to improve stability and interpretability of estimates. This enables a more quantitative analysis focused on the strength rather than the mere presence of differential expression. Expression level difference analysis is a statistical inference process to determine the occurrence of differential expression of all detected genes. Due to the large number of genes involved, statistical tests need to be performed multiple times (the number of genes to be tested). In order to control the false discover rate, the pvalue obtained from statistical tests is need corrected, which perform multiple correct tests. Then the p-adjust value smaller than 0.05 was significant. With EDSeq2, the Wald test is commonly used for hypothesis testing when comparing two groups. A Wald test statistic is computed along with a probability that a test statistic at least as extreme as the observed value were selected at random. This probability is called the p-value of the test. Use software Goatools to perform GO enrichment analysis on the genes in the gene set, so as to obtain the main GO functions of the genes in the gene set. The method of use is Fisher's exact test. When the corrected P value (p-adjust) < 0.05, the GO function is considered to be significantly enriched. Use the R script to perform KEGG PATHWAY enrichment analysis on the genes in the gene set. The calculation principle is the same as the GO function enrichment analysis. When the corrected P value (p-adjust) < 0.05, the KEGG PATHWAY function is considered to be significantly enriched. RT-PCR data were analyzed by using unpaired 2-tailed Student's t tests; $p < 0.05$ (*), $p < 0.01$ (**). Data were expressed as mean ± S.E.M (standard error of mean).

Result

Identification and Characteristicsof circRNAs

To perform comprehensive profiling of circular RNA in pigs, we performed total RNA sequencing in three major organs/tissues of lipid anabolic metabolism (fat, liver, and skeletal muscle) and across four developmental stages (30, 90, 150 and 210 dafter birth) in pigs. In this study, after low-quality and adapter-polluted reads were first removed from the raw data, the Q30 value of the clean reads of the three organs/tissues at 30, 90, 150, and 210 d was observed to be greater than 95% (Table 1). Among the samples, as mapped with the Ningxiang pig genome (accession number PPJNA531381)assembled by our research group, the mapping rate of each sample exceeded 92%.In addition, HISAT was used for sequence segmentation alignment to accurately identify circRNAs. We identified 61,683 unique circRNAs in all assessed biological tissues (Additional Table S1).Analysis of chromosome distribution indicated that the identified circRNAs were transcribed widely and unevenly on the chromosome. Compared with other chromosomes, most of the circRNAs to be identified were distributed on chromosome 1, chromosome 6 and chromosome 13, which is in keeping with the characteristics of circRNAs reported by others[17].In addition, we also detected circRNAs in the sex chromosomes (Fig. 1A).As shown in previous studies, most circRNAs contain multiple exons, and some circRNAs also retain introns. In this study, most of the circRNAs identified (approximately 68.6–69.7%) were exons followed by intergenic circRNAs (approximately 16.1–17.8%), and only a small portion (approximately 12.8–15.3%) were located in introns. The length analysis showed that most circRNAs in the three tissues were longer than 3000 bp (Fig. 1B). We further constructed Venn diagrams of the identified circRNAs in three tissues and at four time points (Fig. 1D-1E). We found that a total of 9563 circRNAs were coexpressed in the three tissues, but the number of circRNAs uniquely expressed in the liver was considerably greater than that in muscle and fat. At the same time, it was found that a total of 9202 circRNAs were coexpressed in the four time periods. However, the number of circRNAs identified at 90 d was the largest, and the number of circRNAs that were uniquely expressed at 90 d was notably greater than that at other time points. CircRNAs also showed tissue-specific and time-specific expression in skeletal muscle, fat, and liver during the development of Ningxiang pigs.

Table 1
Sequencing basic data of four different developmental stages of Ningxiang pig three organs/tissues

Terms	NX30d			NX90d			NX150d			NX210d	
	Muscle	Fat	Live	Muscle	Fat	Live	Muscle	Fat	Live	Muscle	F
Raw reads number	65606883	57278618	56500489	50488816	53672934	55531984	53929255	45120232	45030983	56107588	5
Clean reads number	64137048	56517482	55574608	48897656	52575561	54755520	52912480	44451010	44381475	55237321	5
Clean reads rate	97.76%	98.67%	98.36%	96.85%	97.96%	98.60%	98.11%	98.52%	98.56%	98.45%	9
Clean Q30 bases rate	95.42%	95.02%	95.14%	95.35%	95.48%	95.55%	95.35%	95.48%	95.28%	95.63%	9
Mapped reads	120386916	106157588	102827570	91329628	97298423	103499271	99877320	81793231	83368071	104372240	1
Mapping rate	93.85%	93.90%	92.51%	93.38%	92.55%	94.51%	94.38%	92.00%	93.92%	94.48%	9

The values represent the reads and proportion that were compared to those in the Ningxiang pig reference genome (PRJNA531381) using the Hisat2 program

Expression Pattern of circRNAs in the Muscle Growth and Development of NingxiangPigs

Intramuscular fat (IMF) content and fatty acid composition are important meat quality characteristics[18]. However, the molecular mechanisms regulating intramuscular fat accumulation and fatty acid composition have not been fully elucidated. To understand the regulation of circRNAs in skeletal muscle, we analyzed the expression profile of circRNAs in skeletal muscle at 30, 90, 150 and 210 d after birth. This analysis can assess the dynamic changes in circRNA expression from lactation to fattening and identify circRNAs that may be related to intramuscular fat (IMF) deposition and fatty acid composition. First, we designed five comparison groups (1:30 d vs. 90 d; 2: 30d vs. 150 d; 3: 30d vs. 210 d; 4: 90 d vs. 150 d; and 5: 150 d vs 210 d) to characterize the differential expression of circRNAs (DECs) during development. Differentially expressed circRNAs were identified by DEseq2with P-values < 0.05 and fold-changes > 2 between any two groups. A total of 1786 circRNAs were defined as DECs among these comparison groups (Fig. 2A).

Next, we attempted to evaluate the potential functions of differentially expressed circRNAs (DECs) between two closed time points. Compared with piglets (30 d after birth), among these DECs, 156 circRNAs were upregulated at 90d, 204 circRNAs were upregulated at 150 d, and 188 circRNAs were upregulated at 210 d (Fig. 2B, Additional Table S2).Under the assumption that the functions of circRNAs are related to the functions of their host genes, we performed KEGG pathway analysis to predict the functions of DECs during the growth and development of skeletal muscle. KEGG pathway analysis showed that compared with the lactation period (30 d), the biological functions of these three closed time points were different. For example, in skeletal muscle, significantly upregulated pathways at 90d are primarily involved in such processes as propanoate metabolism, valine, leucine and isoleucine degradation, and starch and sucrose metabolism; the significantly upregulated pathways at 150dare primarily involved in such processes as ubiquitin-mediated proteolysis, cellular senescence, and starch and sucrose metabolism; the significantly upregulated pathways at 210d are primarily related to genetic information processing, including such processes as RNA degradation, ubiquitin-mediated proteolysis, and protein processing in the endoplasmic reticulum. However, the downregulated pathways of these three groups of closed time points are all related to lipid metabolism and transport, including such processes as fatty acid biosynthesis, primary bile acid biosynthesis, and unsaturated fatty acid and peroxisome biosynthesis($p < 0.05$, Additional Fig. 1 and Additional Table S3).Overall, studies of the host genes of DECs at various time points indicate that the circularization of these genes may be important for skeletal muscle function. Among these circRNAs, we also found that 55were identified as common DE genes throughout the muscle development process (Fig. 2C and Additional TableS4).These common DE genes play important roles in development. KEGG pathway analysis indicated that these common DE genes were mainly enriched in lysosomes, cellular senescence, the VEGF signaling pathway, and ABC transporters(Fig. 2D).

To study the role of circRNAs in the transformation of skeletal muscle function, in addition to 30 d vs 90 d, we added 90d vs 150 d and 150 d vs 210 d comparisons. The results represent circRNAs that were up- or downregulated only between two consecutive time points during muscle growth. Between 90d and 150 d, the significantly upregulated pathways were primarily involved in such processes as longevity regulation, EGFR tyrosine kinase inhibitor resistance, and lysine degradation, and the downregulated pathways were primarily involved in such processes as valine, leucine and isoleucine degradation, ubiquitin-mediated proteolysis, and regulation of actin cytoskeleton. Compared with the results obtained at 150d, the pathways upregulated at 210d were determined to beprimarily related to rheumatoid arthritis, antigen processing and presentation, and cytokine-cytokine receptor interactions, and downregulated pathways were observed to be primarily related to such metabolic pathways as starch and sucrose metabolism, ketone body synthesis and degradation, and valine, leucine and isoleucine degradation ($p < 0.05$, Additional Fig. 1 and Additional Table S3).These up- and downregulated circRNAs at different time periods may be associated with regulating the initiation or termination of growth and/or physiological processes at specific developmental stages.

Next, we focused on the changing rules of the 20 most abundant circRNAs in skeletal muscle. Notably, several of the most abundant circRNAs in skeletal muscle originate from protein-coding genes with pivotal roles in skeletal muscle growth, intramuscular fat deposition, and intramuscular sugar metabolism (e.g.,*MYH2, MYH6, TTN, PFKFB1, TNNI2*, *MYBPC1*, and *PRKAR1A*) (Fig. 2E and Additional Table S5).

Expression Pattern of circRNAs in the Adipose Tissue Growth and Development of NingxiangPigs

Adipose tissue is primarily composed of fatty acids (FAs) and triglycerides, which play important roles in the quality of meat[19]. However, the type and proportion of fatty acids (FAs) are also affected by such factors as breed and genetic conditions[20, 21].We clustered 3,116 differential circRNAs identified in the five comparison groups to obtain an overview of DECs in adipose tissue (Fig. 3A).

Among these closed time points, we detected 274 circRNAs upregulated at 90 d, 392 circRNAs upregulated at 150 d, and 396 circRNAs upregulated at 210 d compared with 30 d (Fig. 3B and Additional Table S6).KEGG analysis showed that compared with the lactation period (30 d), the upregulated pathways at these three closed time points were significantly enriched in the AMPK signaling pathway. Thesehost genes primarily include*PIK3R1*, *IGF1R*, *PPP2R3A*, *PPARG*, *RPS6KB1*, *ACACA*, and *PPP2R3A*, which encode proteins associated with adipocyte development and lipid anabolism. However, the downregulated KEGG pathways of these three groups of closed time points are all related to such pathways as complement and coagulation cascades, fatty acid biosynthesis, and steroid hormone biosynthesis. In addition, between 90d and 150d, significantly upregulated pathways are primarily involved in such pathways as synthesis and degradation of ketone bodies, synthesis of basal transcription factors, and acute myeloid leukemia, and downregulated pathways are primarily involved in such pathways as complement and coagulation cascades, steroid hormone biosynthesis, and primary bile acid biosynthesis. Compared with 150d, the upregulated pathways at 210d are primarily related to such metabolic pathways as the citrate cycle (TCA cycle), lysine degradation and glutathione metabolism, and downregulated pathways are primarily related to such pathways as protein processing in the endoplasmic reticulum, starch and sucrose metabolism, and adherens junctions($p < 0.05$, Additional Fig. 1 and Additional TableS3).

Compared to piglets at30 d, 256 circRNAs were identified as common DE genes during the entire development process of adipose tissue, indicating that the KEGG pathways were primarily enriched in the complement and coagulation cascades, lysine degradation, the PPAR signaling pathway, the TGF-beta signaling pathway, the AMPK signaling pathway, and the PI3K-Akt signaling pathway (Fig. 3C-3D and Additional Table S7). Among the most abundant circRNAs expressed in adipose tissue, several circRNAs derived from protein-coding genes that affect the key roles of adipose tissue development and fatty acid metabolism are highly expressed in adipose tissue (e.g., NADP-dependent malic enzyme (*ME1*), protein kinase A type 1-α regulatory subunit (*PRKAR1A*),and6-phosphofructo-2-kinase/fructose-2,6-bisphosphatase 1 (*PFKFB1*) (Fig. 3E and Additional TableS8).

Spatiotemporal Dynamic Expression Pattern of circRNAs in the Liver of Ningxiang Pigs

The liver is the primary organ for triglyceride metabolism, and it plays a role as a regulator of energy metabolism together with adipose tissue. The liver regulates the expression of various lipid metabolism-related genes and takes up extracellular free fatty acids to promote the transmembrane transport of fatty acids. To understand the regulation of circRNAs in the liver, we performed expression profiling of circRNAs in the liver at postnatal days 30, 90, 150, and 210. This profiling enabled the evaluation of dynamic changes in circRNA expression from lactation to fattening and the identification of circRNAs associated with fatty acid anabolism and transport.

We clustered the 3,362 differential circRNAs identified in the five comparison groups (Fig. 4A). Between the two closed time points, we detected 598 circRNAs upregulated at 90 d, 580 circRNAs upregulated at 150 d, and 572 circRNAs upregulated at 210 d compared with 30 d(Fig. 4C and Additional TableS9). KEGG analysis showed that between the two closed time points in liver tissue, the significantly upregulated pathways were primarily enriched in lipid metabolism and amino acid metabolism, including such pathways as tryptophan metabolism, primary bile acid biosynthesis, valine, leucine and isoleucine degradation, and retinol metabolism. However, the significantly downregulated pathways were primarily related to signal transduction, such as the Notch signaling pathway, ECM-receptor interactions, and the MAPK signaling pathway ($p < 0.05$, Additional Fig. 1 and Additional TableS3).

In addition, between two consecutive time points, the number of differentially expressed circRNAs in the 90 d vs. 150 d and 150 d vs. 210 d groups was notably lower than that in the 30 d vs. 90 d groups(Fig. 4B). The KEGG pathway analysis also showed that the circRNAs expressed between 30d and 90 d participated in more biological pathways or more complex biological processes ($p < 0.05$, Additional Fig. 1 and Additional TableS3). These results indicate that during liver development, circRNAs may play important roles in the regulation of amino acid metabolism, fatty acid metabolism and carbohydrate metabolism.

Compared to 30d, 559 circRNAs were identified as common DE genes during the entire liver development process, notably exceeding the number of muscle and adipose tissues (Fig. 4D, Additional TableS10). KEGG pathway analysis also indicated that these common DE genes were primarily enriched in such pathways as complement and coagulation cascades, ECM-receptor interactions, tryptophan metabolism, the Notch signaling pathway, and steroid hormone biosynthesis. Next, we observed that several of the most abundant circRNAs in the liver originate from protein-coding genes that play pivotal roles in lipid synthesis and metabolism.(e.g.,Scaffold180_2562774_2570664,Scaffold155_4811844_4828350,and Chr01_143206410_143210729) (Fig. 4E and Additional TableS11).

Construction of the circRNA-miRNA-mRNA coexpression networks through time-series analysis

According to the dynamic expression patterns of the circRNAs across the four developmental stages, we found that all the identified circRNAs were classified into 4, 4 and 5 cluster profiles in the muscle, fat, and liver, respectively. Each tissue included at least 5 significantly enriched model profiles(Fig. 5A-5C). Finally, we observed colored modules and only considered the largest module. Functional enrichment analysis showed that the largest module in the three tissues was enriched in a variety of biological processes. Some of these processes were related to signal transduction, cell growth and death, amino acid metabolism, and lipid metabolism(Additional Table S12).

Previous studies have shown that circRNAs act as miRNA sponges and indirectly regulate gene transcription. To explore whether there are ceRNAs with functional correlations or regulatory relationships between circRNAs that are strongly correlated with time points, we performed STEM analysis of miRNAs and mRNAs(AdditionalFigure2). In the circRNA STEM analysis, we selected the circRNAs in the colored modules to predict the miRNA and obtained the intersection with the miRNAs that are significant in the miRNA STEM analysis. Next, target analysis was performed with mRNAs that are significant in mRNA STEM analysis. We screened 2384 (fat), 2672 (muscle) and 9187 (liver) circRNA-miRNA-mRNA network pairs related to developmental time changes (Additional Table S13). We found that there were far more ceRNA network pairs in the liver than in muscle and fat. More importantly, we identified numerous ceRNA network pairs related tothe cell cycle, cell differentiation, fatty acid biosynthesis metabolism markers, such as *CDK16*, *MYH3*, *ACSL3*, *ACSL5*, *APOA4*, and *FADS*. (Fig. 5D-5F). This result indicates that these ceRNA networks may play an important role in the regulation of adipogenesis and metabolism during the development of Ningxiang pigs.

Verification of Identified circRNAs

To validate the circRNAs identified from the circRNA-Seq analysis, reverse transcription RT-PCR and Sanger sequencing experiments were performed for 11 randomly selected circRNAs. A pair of divergent primers were designed for each circRNA, and both cDNA and gDNA (negative control) were employed as templates for PCR amplification (Fig. 6 and Additional Table S14). Finally, among the 11circRNAs, 10 were successfully confirmed (90.90%), suggesting the reliability of our circRNA identification results. In addition, as an alternative visualization method, we employed fluorescence *in situ* hybridization (FISH) for higher resolution subcellular localization of Chr01_143206410_143210729. At four time points of development, the Chr01_143206410_143210729 signal may be related to both the nucleus and cytoplasm. Although signal strength cannot be utilized as a quantitative measure of circRNA abundance, we detected greater signal strength at 90 d and 150 d, which is consistent with the Chr01_143206410_143210729 sequencing data in muscle(Fig. 6C and Fig. 4E).

Discussion

CircRNAs have been reported to be abundant in animal transcriptomes, and a large number of circRNAs have been identified in humans[22], mice[23], and nematodes[24].Pigs are important farm animals that provide meat for humans and represent an important animal modelfor medical research, and increasing numbers of studies have been conducted on pigs in recent years. Liang et al.[17] identified 149 circRNAs that may be related to muscle growth in the analysis of nine organs and three developmental stages of the Guizhou minipig and found that the host genes of these circRNAs were significantly involved in muscle development and function. These researchers alsoconstructed the first public *S. scrofa*circRNA database[17]. Morten et al. [25]profiled the expression of circRNA in five brain tissues at up to six time points during fetal porcine development, constituting the first report of circRNA in the brain development of a large animal. An unbiased analysis identified a highly complex regulation pattern of thousands of circRNAs with a distinct spatiotemporal expression profile, suggesting the important function of circRNAs in mammalian brain development. Accurate timing of gene expression is highly important for the developmental stage. Because circRNAs are expressed in a highly spatiotemporally specific manner, it is essential that studies of circRNAs in mammals assess various tissues, conditions, and developmental stages. Ningxiang pigs are known for their delicious meat, but the internal control mechanism governing this property have not been elucidated. To study the spatiotemporal expression pattern of circRNA on lipid synthesis, metabolism and transport in Ningxiang pig tissues, we performed total RNA sequencing across three organs (liver, skeletal muscle, and subcutaneous fat)at four developmental stages (30, 90, 150 and 240 d after birth). Compared with the reference genomes of other pig species, the results of using the Ningxiang pig genome assembled by our research group were more robust (data not published). The mapping rate of each sample exceeded 92%, and the percentage of Q30 bases was more than 92% (Table 1). We identified 61,683 circRNAs in all evaluated tissues. The identified circRNAs had similar distribution trends in chromosome, number, and length among the three tissues. As indicated in a previous study[17], more circRNAs were generated from chromosome 1, chromosome 6 and chromosome 13 than from the other chromosomes, and the largest number was derived from exons. In addition, the number of circRNAs identified at 90d was the largest, and the number of uniquely expressed circRNAs at 90 d was considerably greater than that at other time points. We also identified tissue-specific circular RNAs, which provided important information regarding their functions. For example, we identified 13871, 6274 and 20646 tissue-specific circRNAs in muscle, fat and liver, respectively(Fig. 1C). These findings suggest that specifically expressed circRNAs may play specific roles at specific times during the development of tissues or organs. This possibility is consistent with the findings of other studies, indicating that circRNAs have tissue-/stage-specific expression differences[25–27]. Subsequently, the identification of circRNAs by grouping statistics indicated that 3,362, 1,786 and 3,116 circRNAs with significant differential expression in Ningxiang pig liver, muscle and adipose tissue, respectively.

Since the number of muscle fibers has been determined after birth, skeletal muscle mass increases during postnatal development through a process of hypertrophy, and a similar process may be induced in adult skeletal muscle in response to contractile activity[28]. Each skeletal muscle in an animal contains a different type of fiber. Type I muscle fibers are rich in mitochondria and have a higher oxidative metabolism, while type IIB fibers have fewer mitochondria, and the glycolytic metabolism capacity is higher[29]. However, the role of circRNAs in skeletal muscle development is unknown. The identified circRNAs that were abundantly expressed in muscle include Chr05_81425549_81426478, Chr15_85761324_85761662, Scaffold180_2562774_2570664, Chr02_159842602_159843286, and Chr12_55773288_55775037(Fig. 2E and Additional Table S5). The contractile protein troponin I (*TnI*), a constituent protein of the troponin complex located on the thin filaments of striated muscle, is involved in calcium-mediated contraction and relaxation. Vertebrate *TnI* has evolved into three isoforms encoded by three homologous genes, which are expressed under muscle type-specific and developmental regulatory mechanisms[30, 31]. Among these genes, *TNNI2* (fast-twitch skeletal muscle isoform, named TNI-fast) is a specific protein of the fast muscle fiber type. During muscle development, Chr02_159842602_159843286, produced by the host gene *TNNI2*, was abundantly expressed at 30d.It has been reported that the change in*MYBPC1* abundance is related to the production of slow-twitch muscle fibers[32, 33]. Interestingly, we observed a peak expression of Chr05_81425549_81426478 transcribed by myosin binding protein C1 (*MYBPC1*) as a host gene in the developing 90 d pig muscle.Chr15_85761324_85761662, produced by the host gene titin (*TTN*), was demonstrated to be expressed at 30d and reached its peak at 210 d. It has been reported that *TTN* is related to intramuscular fat deposition[34], and recent studies have found that the circular RNA *TTN* acts as a miR-432 sponge to facilitate the proliferation and differentiation of cattle myoblasts via the IGF2/PI3K/AKT signaling pathway[35].In addition, the most abundant circRNAs expressed in muscles are also derived from members of the *MYH* myosin superfamily, such as *MYH2* and *MYH6*. Recent studies have shown that these genes

are associated with skeletal muscle development and influence the quality of pork[36]. These findings suggest that many circRNAs exhibit different expression patterns during muscle development, and changes in the abundance of these circRNAs may affect muscle fiber composition, thereby affecting the properties of meat. Notably, pathway analysis of the genes giving rise to circRNAs peaking at 30d indicated a significant predominance of genes associated with fatty acid biosynthesis, primary bile acid biosynthesis, unsaturated fatty acid biosynthesis, and peroxisome biosynthesis. The impact of circRNAs on the biosynthesis of unsaturated fatty acids will be of great concern and may be related to the higher proportion of unsaturated fatty acids in the diet of piglets. Malic enzyme 1 (*ME1*) plays an important role in the Krebs cycle for energy metabolism. The mRNA of *ME1* was observed to be more abundant in obese Rongchang pigs than in lean Landrace pigs. Furthermore, mRNA abundance changes in ME1 have a marked significant positive correlation with adipocyte volume across the six adipose tissue types[37]. Chr01_176448874_176466186 is produced by the host gene ME1, which is abundantly expressed in adipose tissue (Fig. 3E and Additional TableS8). The expression of Chr01_176448874_176466186 was shown to increase from 90 d, peaking at 150 d and subsequently, with fluctuations, decrease until 210 d. This gene is surmised to be closely related to adipocyte development and adipodeposition. CircRNAs may also be involved in lipid transport; for example, Scaffold155_4811844_4828350 is abundantly expressed in the liver at 90d, and its host gene integer alpha-9 (*ITGA9*) is known to participate in the sphingolipid pathway(Fig. 4E and Additional TableS11).These lipids are required for active transport, a number of enzymatic processes, membrane formation, and cell signaling[38]. Fructose 2,6-bisphosphate (Fru-2,6-P2) is an important metabolite that controls glycolytic and gluconeogenic pathways in several cell types. The synthesisand degradation of this metabolite are catalyzed by the bifunctional enzyme 6-phosphofructo-2-kinase/fructose 2,6-bisphosphatase (*PFKFB1*)[39, 40]. Due to the abundant expression of Scaffold180_2562774_2570664 produced by the host gene *PFKFB1* in muscle and liver, we surmise that Scaffold180_2562774_2570664 may affect the accumulation of lipids by participating in the regulation of the activity of related metabolic enzymes in gluconeogenesis during muscle and liver development, but this possibility requires follow-up experimental verification. In addition, we found that Chr01_143206410_143210729 was abundantly expressed in all three organs but presented different expression patterns. For example, the expression of Chr01_143206410_143210729 in developmental adipose tissue was shown to increase from 30 d, peak at 150 d and subsequently, with fluctuations, decrease towards 210 d. However, the expression of Chr01_143206410_143210729 in muscle and liver peaked at 90 d and decreased gradually thereafter. Although Chr01_143206410_143210729's host gene SAFB-like transcription modulator(*SLTM*) has rarely been reported, its homologous family member *SAFB1*can interact with and repress the transcriptional activity of various other nuclear receptors, including *PPARγ, FXRα, RORα1, PPARα, PPARβ, VDR, SF1*, and *LRH-1*[41]. *SAFB1* was also shown to regulate the expression of *SREBP-1c*, a bHLH transcription factor that controls lipogenesis in the liver and is induced during over nutrition to facilitate the conversion of glucose to fatty acids and triglycerides for the storage of excess energy[42]. *SLTM* shares 34% overall identity with *SAFB1*. *SLTM* contains SAP and RRM domains, which share higher similarities of 60% and 70%, respectively, with *SAFB1*[43, 44]. The presence of these shared domains suggests at least some common functions between *SAFB1* and *STLM*; however, it is reasonable to suspect that the circularization of these genes may play important roles in the additive, synergistic, or potentially antagonistic functions exhibited by family members.

Time-series analysis showed that certain differential circRNAs are dynamically expressed during skeletal muscle, liver and adipose tissue development. Although the molecular function of circRNAshas not been fully elucidated, the current research shows that in addition to the function of circRNAs in regulating host gene transcription, protein binding and translation, further research is needed to determine the role of miRNA sponges[45, 46].Competing endogenous RNAs (ceRNAs) are widely present in muscle, fat, and liver. For example, circular RNA*SNX29* sponges miR-744 to regulate the proliferation and differentiation of myoblasts by activating the Wnt5a/Ca signaling pathway[47]. CircSAMD4A regulates preadipocyte differentiation by acting as a miR-138-5p sponge and thus increasing *EZH2* expression[48]. CircRNA_0046366 inhibits hepatocellular steatosis by abolishing the miR-34a-dependent inhibition of *PPARα*[49]. In our study, STEM analysis and ceRNA analysis were combined to screen out the interaction network pairs closely related to time point changes. For example, G protein signaling 9 (*RGS9*) is the targeted gene of ssc-miRNA-7137-3p, while the miRNA targeted 8 circRNAs(Chr15_57751128_57770746, Chr14_24730872_24760271, Chr03_19654503_19689919, Chr11_10784978_10824218, Chr06_124537421_124559486, Chr08_82174982_82248693, Chr07_23444137_23455147, Chr12_24249907_24258995) (Fig. 5D and Additional Table S13) in the muscle network diagram. As reported, RGS 9 knockout mice showed higher body weight and greater fat accumulation than wild-type mice[50, 51]. In addition, we also identified numerous well-known key markers in the muscle ceRNA networks, e.g., *CDK16*, *CYC1*, *MYH3*, *HDC*, and *E2F1* for muscle cell growth and differentiation and *FAAH*, *PLIN3*, *PNPLA2*, and *GAS7* for lipid synthesis and metabolism[52–54], suggesting that these ceRNA networks may play critical roles during muscle growth and development processes and providing ideas for further research studying muscle development and intramuscular fat deposition.

The differentiation of adipocytes is a highly complex biological process. While regulated by a series of transcription factor cascades, various cytokines can also participate in initiating and regulating the differentiation of adipocytes and maintaining cell characteristics through complex signal transduction. Adipose tissue is also an active endocrine organ that can secrete some hormones or cytokines (e.g., resistin, tumor necrosis factor-α and complement D) to participate in the immune response and treatment of obesity or cardiovascular diseases and other physiological and pathological processes[55, 56]. However, these functions may be inseparable from the regulation of circRNAs. For example, in our study, Chr15_78588493_78637426, produced by *TLK1* as the host gene, was abundantly expressed in adipose tissue, starting at 30 d and decreasing after peaking at 150 d (Fig. 3E and Additional TableS8). Tousled-like kinase 1 (*TLK1*) is a serine/threonine protein kinase that is implicated in chromatin remodeling, DNA replication and mitosis[57]. Combined with the joint analysis results of SETM and ceRNA, it was found that among the predicted target miRNAs of circRNA-TLK1, only miRNA-204 was significantly expressed in the STEM analysis of miRNA. Among the target mRNAs of miRNA-204, only 4 mRNAs (*LALMA4, COL6A1, ABCD2, ELMOD3*) were significantly expressed in mRNA STEM analysis(Additional TableS13). It has been reported that lamininα4 (*LAMA4*) is located in the extracellular basement membrane that surrounds each individual adipocyte and affects the structure and function of adipose tissue in a depot-specific manner. Compared with wild-type (WT) mice, *LAMA4*$^{-/-}$ mice showed higher energy expenditure at room temperature and when exposed to a cold challenge. In addition, the mice had decreased adipose tissue mass and altered lipogenesis in a depot-specific manner[58, 59]. Interestingly, some scientists believe that obesity is an inflammatory condition that is associated with increased extracellular matrix (ECM) gene expression, whereas the collagen 6A1(*COL6A1*) gene is the primary gene in the ECM[60]. The ATP-binding cassette transporter*ABCD2* (*D2*) is a peroxisomal protein whose mRNA is highly expressed in fat and upregulated during adipogenesis. There are also articles reporting that *D2* can not only promote the oxidation of long-chain monounsaturated fatty acids (LCMUFAs) but also inhibit the accumulation of dietary erucic acid (EA, 22:1ω9) in fat cells[61, 62]. These findings indicate that the same circRNA may play different roles in fat development and function.

Interestingly, combined with STEM analysis, we identified more ceRNA network pairs in the liver than in muscle and fat. Among these transcripts, many target mRNAs were determined to be related to fat metabolism and transport, such as *ACSL3*, *ACSL5*, *APOA4*, and *PLIN4*, and *FADS*, *HACD3*, and *ACACA*, for unsaturated fatty acid synthesis, indicating that these circRNAs are involved in fatty acid synthesis, metabolism and transport during the development of liver tissue. These results indicate that these ceRNA networks are active throughout tissue development. Although these *in silico* results should be investigated further *in vivo*, these results imply functional relatedness or a regulatory relationship between circRNAs and miRNAs during tissue development.

Conclusions

This study provides a clear and accurate dynamic profile of circRNAs in skeletal muscle, subcutaneous fat and liver based on our Ningxiang pig genome. Moreover, our study helps to elucidate the role played by circRNAs in lipid synthesis and metabolism and provides high-quality resources and new ideas for further research studying the molecular mechanism governing pork quality traits.

Abbreviations

ncRNA, non-coding RNA; lncRNA, long non-coding RNA; miRNA, microRNA; circRNAs, circular RNAs; 30d, 30 day; 90d, 90 day; 210d, 210 day; vs, versus; DEGs, Differentially expressed mRNAs; ceRNA, Competitive endogenous RNA; DECs, Differentially expressed circRNAs; FDR, False discovery rate; TPM, Transcripts Per Kilobase of exon model per Million mapped reads; KEGG, Kyoto Encyclopedia of Genes and Genomes; STEM, Short Time-series Expression Miner; RPM Reads per million mapped reads; RNA-Seq, RNA sequencing; CIRI 2, CircRNA identifier 2; WGCNA, Weighted Gene Co-Expression Network Analysis;

Declarations

Funding

This study was supported by Genetic resource innovations and its application of indigenous pig breeds in Hunan province (2019NK2193), "double first Class" Construction Project of Hunan Agricultural University (kxk201801004), Strategic Priority Research Program of Chinese Academy of Sciences (XDA24030204), National Natural Science Foundation of China (U19A2037), Basic Research Project of Ningxiang Pig(15073), Hunan Natural Science Joint Fund(2018JJ4003) and Hunan Science and Technology Innovation Project(72010102-30218).

Availability of data and materials

The datasets used and analyzed during the current study are available from the corresponding author on reasonable request.

Authors' contributions

B. L. performed data analysis and wrote the manuscript. Q. Z. and J. H. provided the site of experiment and some of test conditions support. Y. Z. and Y. G. conducted part of animal experiments. Y. X completed the animal feeding experiment. K. X., J. H. and H. M. designed this study and revised the manuscript.

Ethics approval

All animal experiments in this study were approved by the “Institutional Animal Care and Use Committee of Hunan Agricultural University”(Changsha, China).

Consent for publication

Not applicable.

Competing Interest

The authors have no conflicts of interest to declare.

Acknowledgements

We thank the following: Mr. Yan Gong, Mrs. Yu Xiao and Mrs. Shishu Ying in College of Animal Science and Technology, Hunan Agricultural University, for their assistances and valuable suggestions during the experiment and manuscript writing.

References

1. Sun J, Xie M, Huang Z, Li H, Chen T, Sun R, Wang J, Xi QY, Wu T, Zhang Y: **Integrated analysis of non-coding RNA and mRNA expression profiles of 2 pig breeds differing in muscle traits**. *Journal of animal science* 2017, **95**(3):1092-1103.
2. Jiang QM, Li CY, Yu YN, Xing YT, Xiao DF, Zhang B: **Comparison of fatty acid profile of three adipose tissues in Ningxiang pigs**. *Anim Nutr* 2018, **4**(3):256-259.
3. He QH, Ren PP, Kong XF, Wu YN, Wu GY, Li P, Hao FH, Tang HR, Blachier F, Yin YL: **Comparison of serum metabolite compositions between obese and lean growing pigs using an NMR-based metabonomic approach**. *J Nutr Biochem* 2012, **23**(2):133-139.
4. Schmitz G, Ecker J: **The opposing effects of n-3 and n-6 fatty acids**. *Progress in lipid research* 2008, **47**(2):147-155.
5. Saravanan P, Davidson NC, Schmidt EB, Calder PC: **Cardiovascular effects of marine omega-3 fatty acids**. *Lancet* 2010, **376**(9740):540-550.

6. Gerfault V, Louveau I, Mourot J, Le Dividich J: **Lipogenic enzyme activities in subcutaneous adipose tissue and skeletal muscle from neonatal pigs consuming maternal or formula milk**. *Reproduction, nutrition, development* 2000, **40**(2):103-112.
7. Boone C, Mourot J, Gregoire F, Remacle C: **The adipose conversion process: regulation by extracellular and intracellular factors**. *Reproduction, nutrition, development* 2000, **40**(4):325-358.
8. Kershaw EE, Hamm JK, Verhagen LA, Peroni O, Katic M, Flier JS: **Adipose triglyceride lipase: function, regulation by insulin, and comparison with adiponutrin**. *Diabetes* 2006, **55**(1):148-157.
9. Amills M, Vidal O, Varona L, Tomas A, Gil M, Sanchez A, Noguera JL: **Polymorphism of the pig 2,4-dienoyl CoA reductase 1 gene (DECR1) and its association with carcass and meat quality traits**. *Journal of animal science* 2005, **83**(3):493-498.
10. Vidal O, Varona L, Oliver MA, Noguera JL, Sànchez A, Amills M: **Malic enzyme 1 genotype is associated with backfat thickness and meat quality traits in pigs**. *Animal genetics* 2006, **37**(1):28-32.
11. Hansen TB, Jensen TI, Clausen BH, Bramsen JB, Finsen B, Damgaard CK, Kjems J: **Natural RNA circles function as efficient microRNA sponges**. *Nature* 2013, **495**(7441):384-388.
12. Li A, Huang WL, Zhang XX, Xie LL, Miao XY: **Identification and Characterization of CircRNAs of Two Pig Breeds as a New Biomarker in Metabolism-Related Diseases**. *Cellular Physiology and Biochemistry* 2018, **47**(6):2458-2470.
13. Kokta TA, Dodson MV, Gertler A, Hill RA: **Intercellular signaling between adipose tissue and muscle tissue**. *Domestic animal endocrinology* 2004, **27**(4):303-331.
14. Liu CD, Shen LY, Du JJ, Wu XQ, Luo J, Pu Q, Tan ZD, Cheng X, Du JG, Yang Q *et al*: **The effect of lipid metabolism-related genes on intramuscular fat content and fatty acid composition in multiple muscles**. *Anim Prod Sci* 2018, **58**(11):2003-2010.
15. Ernst J, Bar-Joseph Z: **STEM: a tool for the analysis of short time series gene expression data**. *BMC bioinformatics* 2006, **7**:191.
16. Morris JH, Vijay D, Federowicz S, Pico AR, Ferrin TE: **CyAnimator: Simple Animations of Cytoscape Networks**. *F1000Research* 2015, **4**:482.
17. Liang G, Yang Y, Niu G, Tang Z, Li K: **Genome-wide profiling of Sus scrofa circular RNAs across nine organs and three developmental stages**. *DNA research : an international journal for rapid publication of reports on genes and genomes* 2017, **24**(5):523-535.
18. Cameron ND, Enser MB: **Fatty acid composition of lipid in Longissimus dorsi muscle of Duroc and British Landrace pigs and its relationship with eating quality**. *Meat science* 1991, **29**(4):295-307.
19. Delgado GL, Gomez CS, Rubio LM, Capella VS, Mendez MD, Labastida RC: **Fatty acid and triglyceride profiles of intramuscular and subcutaneous fat from fresh and dry-cured hams from Hairless Mexican Pigs**. *Meat science* 2002, **61**(1):61-65.
20. Martins AP, Lopes PA, Madeira MS, Martins SV, Santos NC, Moura TF, Prates JA, Soveral G: **Differences in lipid deposition and adipose membrane biophysical properties from lean and obese pigs under dietary protein restriction**. *Biochemical and biophysical research communications* 2012, **423**(1):170-175.
21. Kouba M, Enser M, Whittington FM, Nute GR, Wood JD: **Effect of a high-linolenic acid diet on lipogenic enzyme activities, fatty acid composition, and meat quality in the growing pig**. *Journal of animal science* 2003, **81**(8):1967-1979.
22. Liu YC, Li JR, Sun CH, Andrews E, Chao RF, Lin FM, Weng SL, Hsu SD, Huang CC, Cheng C *et al*: **CircNet: a database of circular RNAs derived from transcriptome sequencing data**. *Nucleic Acids Res* 2016, **44**(D1):D209-215.
23. Guo JU, Agarwal V, Guo HL, Bartel DP: **Expanded identification and characterization of mammalian circular RNAs**. *Genome biology* 2014, **15**(7).
24. Memczak S, Jens M, Elefsinioti A, Torti F, Krueger J, Rybak A, Maier L, Mackowiak SD, Gregersen LH, Munschauer M *et al*: **Circular RNAs are a large class of animal RNAs with regulatory potency**. *Nature* 2013, **495**(7441):333-338.
25. Veno MT, Hansen TB, Veno ST, Clausen BH, Grebing M, Finsen B, Holm IE, Kjems J: **Spatio-temporal regulation of circular RNA expression during porcine embryonic brain development**. *Genome biology* 2015, **16**.
26. Westholm JO, Miura P, Olson S, Shenker S, Joseph B, Sanfilippo P, Celniker SE, Graveley BR, Lai EC: **Genome-wide Analysis of Drosophila Circular RNAs Reveals Their Structural and Sequence Properties and Age-Dependent Neural Accumulation**. *Cell Rep* 2014, **9**(5):1966-1980.
27. Szabo L, Morey R, Palpant NJ, Wang PL, Afari N, Jiang C, Parast MM, Murry CE, Laurent LC, Salzman J: **Statistically based splicing detection reveals neural enrichment and tissue-specific induction of circular RNA during human fetal development**. *Genome biology* 2015, **16**:126.
28. Schiaffino S, Dyar KA, Ciciliot S, Blaauw B, Sandri M: **Mechanisms regulating skeletal muscle growth and atrophy**. *Febs J* 2013, **280**(17):4294-4314.
29. Zhang L, Zhou Y, Wu W, Hou L, Chen H, Zuo B, Xiong Y, Yang J: **Skeletal Muscle-Specific Overexpression of PGC-1α Induces Fiber-Type Conversion through Enhanced Mitochondrial Respiration and Fatty Acid Oxidation in Mice and Pigs**. *International journal of biological sciences* 2017, **13**(9):1152-1162.
30. Yang H, Xu ZY, Lei MG, Li FE, Deng CY, Xiong YZ, Zuo B: **Association of 3 polymorphisms in porcine troponin I genes (TNNI1 and TNNI2) with meat quality traits**. *Journal of applied genetics* 2010, **51**(1):51-57.
31. Sheng JJ, Jin JP: **TNNI1, TNNI2 and TNNI3: Evolution, regulation, and protein structure-function relationships**. *Gene* 2016, **576**(1 Pt 3):385-394.
32. Tong B, Xing YP, Muramatsu Y, Ohta T, Kose H, Zhou HM, Yamada T: **Association of expression levels in skeletal muscle and a SNP in the MYBPC1 gene with growth-related trait in Japanese Black beef cattle**. *Journal of genetics* 2015, **94**(1):135-137.
33. Chen Z, Zhao TJ, Li J, Gao YS, Meng FG, Yan YB, Zhou HM: **Slow skeletal muscle myosin-binding protein-C (MyBPC1) mediates recruitment of muscle-type creatine kinase (CK) to myosin**. *The Biochemical journal* 2011, **436**(2):437-445.
34. Sasaki Y, Nagai K, Nagata Y, Doronbekov K, Nishimura S, Yoshioka S, Fujita T, Shiga K, Miyake T, Taniguchi Y *et al*: **Exploration of genes showing intramuscular fat deposition-associated expression changes in musculus longissimus muscle**. *Animal genetics* 2006, **37**(1):40-46.

35. Wang XG, Cao XK, Dong D, Shen XM, Cheng J, Jiang R, Yang ZX, Peng SJ, Huang YZ, Lan XY *et al*: **Circular RNA TTN Acts As a miR-432 Sponge to Facilitate Proliferation and Differentiation of Myoblasts via the IGF2/PI3K/AKT Signaling Pathway**. *Mol Ther-Nucl Acids* 2019, **18**:966-980.
36. Xiong X, Liu X, Zhou L, Yang J, Yang B, Ma H, Xie X, Huang Y, Fang S, Xiao S *et al*: **Genome-wide association analysis reveals genetic loci and candidate genes for meat quality traits in Chinese Laiwu pigs**. *Mammalian genome : official journal of the International Mammalian Genome Society* 2015, **26**(3-4):181-190.
37. Zhou SL, Li MZ, Li QH, Guan JQ, Li XW: **Differential expression analysis of porcine MDH1, MDH2 and ME1 genes in adipose tissues**. *Genet Mol Res* 2012, **11**(2):1254-1259.
38. Demirkan A, van Duijn CM, Ugocsai P, Isaacs A, Pramstaller PP, Liebisch G, Wilson JF, Johansson A, Rudan I, Aulchenko YS *et al*: **Genome-Wide Association Study Identifies Novel Loci Associated with Circulating Phospho- and Sphingolipid Concentrations**. *PLoS genetics* 2012, **8**(2).
39. Wu C, Khan SA, Peng LJ, Lange AJ: **Roles for fructose-2,6-bisphosphate in the control of fuel metabolism: beyond its allosteric effects on glycolytic and gluconeogenic enzymes**. *Advances in enzyme regulation* 2006, **46**:72-88.
40. Duran J, Navarro-Sabate A, Pujol A, Perales JC, Manzano A, Obach M, Gomez M, Bartrons R: **Overexpression of ubiquitous 6-phosphofructo-2-kinase in the liver of transgenic mice results in weight gain**. *Biochemical and biophysical research communications* 2008, **365**(2):291-297.
41. Debril MB, Dubuquoy L, Feige JN, Wahli W, Desvergne B, Auwerx J, Gelman L: **Scaffold attachment factor B1 directly interacts with nuclear receptors in living cells and represses transcriptional activity**. *Journal of molecular endocrinology* 2005, **35**(3):503-517.
42. Omura Y, Nishio Y, Takemoto T, Ikeuchi C, Sekine O, Morino K, Maeno Y, Obata T, Ugi S, Maegawa H *et al*: **SAFB1, an RBMX-binding protein, is a newly identified regulator of hepatic SREBP-1c gene**. *Bmb Rep* 2009, **42**(4):232-237.
43. Garee JP, Oesterreich S: **SAFB1's multiple functions in biological control-lots still to be done!***Journal of cellular biochemistry* 2010, **109**(2):312-319.
44. Chan CW, Lee YB, Uney J, Flynn A, Tobias JH, Norman M: **A novel member of the SAF (scaffold attachment factor)-box protein family inhibits gene expression and induces apoptosis**. *The Biochemical journal* 2007, **407**(3):355-362.
45. Jeck WR, Sharpless NE: **Detecting and characterizing circular RNAs**. *Nature biotechnology* 2014, **32**(5):453-461.
46. Li Z, Huang C, Bao C, Chen L, Lin M, Wang X, Zhong G, Yu B, Hu W, Dai L *et al*: **Exon-intron circular RNAs regulate transcription in the nucleus**. *Nature structural & molecular biology* 2015, **22**(3):256-264.
47. Peng S, Song C, Li H, Cao X, Ma Y, Wang X, Huang Y, Lan X, Lei C, Chaogetu B *et al*: **Circular RNA SNX29 Sponges miR-744 to Regulate Proliferation and Differentiation of Myoblasts by Activating the Wnt5a/Ca(2+) Signaling Pathway**. *Molecular therapy Nucleic acids* 2019, **16**:481-493.
48. Liu YJ, Liu HT, Li Y, Mao R, Yang HW, Zhang YC, Zhang Y, Guo PS, Zhan DF, Zhang TT: **Circular RNA SAMD4A controls adipogenesis in obesity through the miR-138-5p/EZH2 axis**. *Theranostics* 2020, **10**(10):4705-4719.
49. Guo XY, Sun F, Chen JN, Wang YQ, Pan Q, Fan JG: **circRNA_0046366 inhibits hepatocellular steatosis by normalization of PPAR signaling**. *World J Gastroentero* 2018, **24**(3):323-337.
50. Walker PD, Jarosz PA, Bouhamdan M, MacKenzie RG: **Effects of gender on locomotor sensitivity to amphetamine, body weight, and fat mass in regulator of G protein signaling 9 (RGS9) knockout mice**. *Physiology & behavior* 2015, **138**:305-312.
51. Waugh JL, Celver J, Sharma M, Dufresne RL, Terzi D, Risch SC, Fairbrother WG, Neve RL, Kane JP, Malloy MJ *et al*: **Association between regulator of G protein signaling 9-2 and body weight**. *PloS one* 2011, **6**(11):e27984.
52. Smirnova E, Goldberg EB, Makarova KS, Lin L, Brown WJ, Jackson CL: **ATGL has a key role in lipid droplet/adiposome degradation in mammalian cells**. *EMBO reports* 2006, **7**(1):106-113.
53. Deutsch DG, Ueda N, Yamamoto S: **The fatty acid amide hydrolase (FAAH)**. *Prostaglandins, leukotrienes, and essential fatty acids* 2002, **66**(2-3):201-210.
54. Yang X, Deignan JL, Qi H, Zhu J, Qian S, Zhong J, Torosyan G, Majid S, Falkard B, Kleinhanz RR *et al*: **Validation of candidate causal genes for obesity that affect shared metabolic pathways and networks**. *Nature genetics* 2009, **41**(4):415-423.
55. Kershaw EE, Flier JS: **Adipose tissue as an endocrine organ**. *The Journal of clinical endocrinology and metabolism* 2004, **89**(6):2548-2556.
56. Oller do Nascimento CM, Ribeiro EB, Oyama LM: **Metabolism and secretory function of white adipose tissue: effect of dietary fat**. *Anais da Academia Brasileira de Ciencias* 2009, **81**(3):453-466.
57. Hashimoto M, Matsui T, Iwabuchi K, Date T: **PKU-beta/TLK1 regulates myosin II activities, and is required for accurate equaled chromosome segregation**. *Mutation research* 2008, **657**(1):63-67.
58. Vaicik MK, Thyboll Kortesmaa J, Movérare-Skrtic S, Kortesmaa J, Soininen R, Bergström G, Ohlsson C, Chong LY, Rozell B, Emont M *et al*: **Laminin α4 deficient mice exhibit decreased capacity for adipose tissue expansion and weight gain**. *PloS one* 2014, **9**(10):e109854.
59. Vaicik MK, Blagajcevic A, Ye H, Morse MC, Yang F, Goddi A, Brey EM, Cohen RN: **The Absence of Laminin α4 in Male Mice Results in Enhanced Energy Expenditure and Increased Beige Subcutaneous Adipose Tissue**. *Endocrinology* 2018, **159**(1):356-367.
60. Adapala VJ, Adedokun SA, Considine RV, Ajuwon KM: **Acute inflammation plays a limited role in the regulation of adipose tissue COL1A1 protein abundance**. *J Nutr Biochem* 2012, **23**(6):567-572.
61. Liu J, Sabeva NS, Bhatnagar S, Li XA, Pujol A, Graf GA: **ABCD2 is abundant in adipose tissue and opposes the accumulation of dietary erucic acid (C22:1) in fat**. *Journal of lipid research* 2010, **51**(1):162-168.
62. Liu J, Liang S, Liu X, Brown JA, Newman KE, Sunkara M, Morris AJ, Bhatnagar S, Li X, Pujol A *et al*: **The absence of ABCD2 sensitizes mice to disruptions in lipid metabolism by dietary erucic acid**. *Journal of lipid research* 2012, **53**(6):1071-1079.

Figures

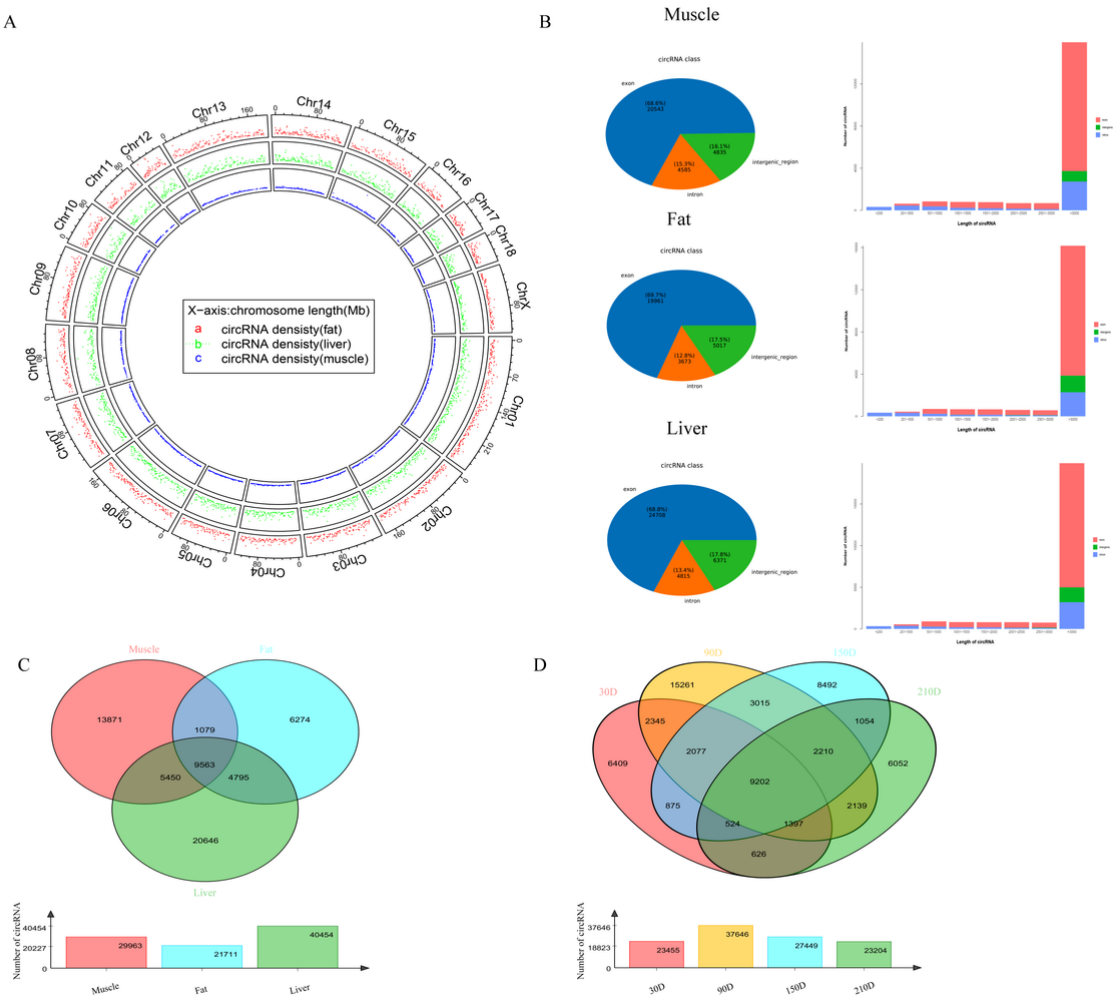

Figure 1

Identification and feature of circRNAs in pigs. (A) Distribution of circRNAs in each chromosome. (B) Genomic location of circRNAs. (C) Length distribution of circRNAs.(D) Venn diagram of circRNAs identified in fat, muscle, and liver tissues of Ningxiang pigs. (E) Venn diagram of circRNAs identified at four development pointsof Ningxiang pigs.

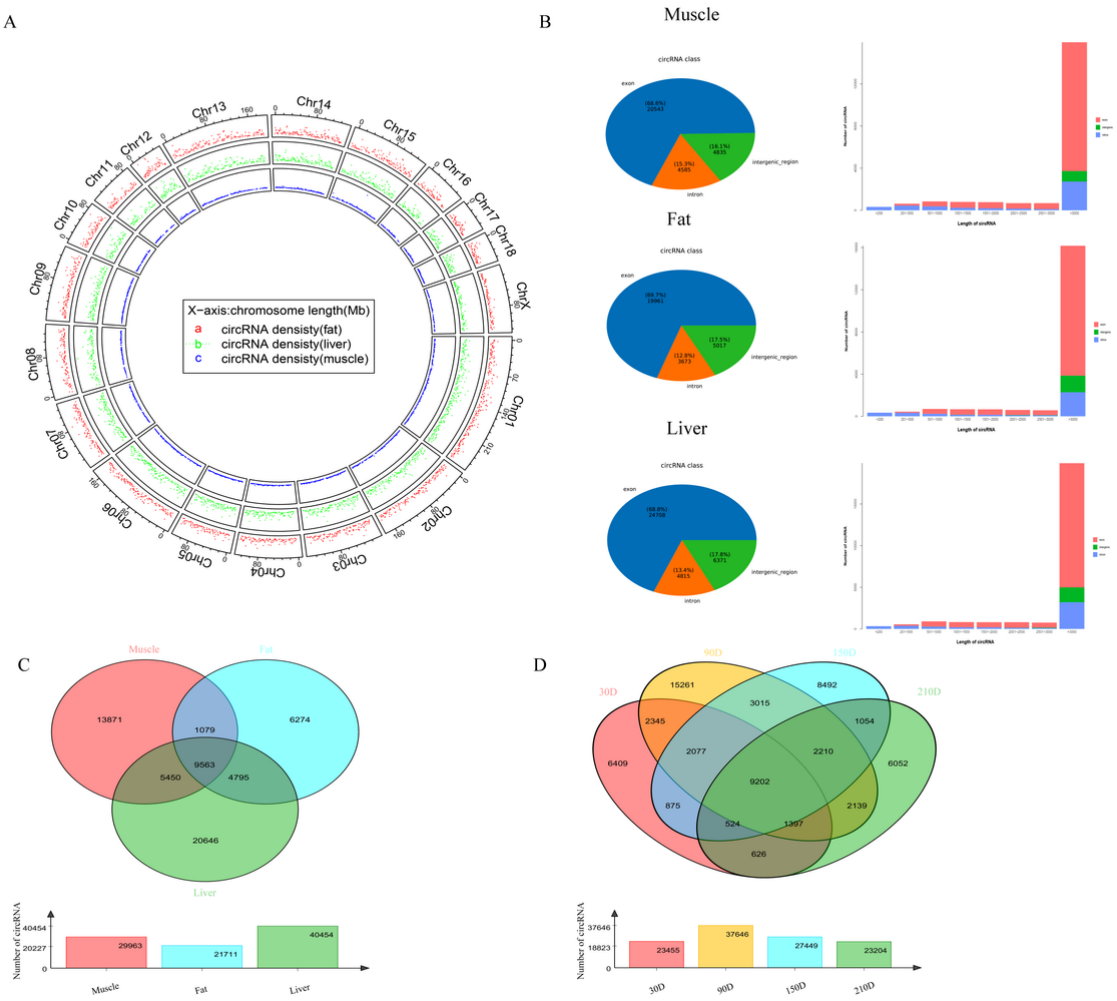

Figure 1

Identification and feature of circRNAs in pigs. (A) Distribution of circRNAs in each chromosome. (B) Genomic location of circRNAs. (C) Length distribution of circRNAs.(D) Venn diagram of circRNAs identified in fat, muscle, and liver tissues of Ningxiang pigs. (E) Venn diagram of circRNAs identified at four development pointsof Ningxiang pigs.

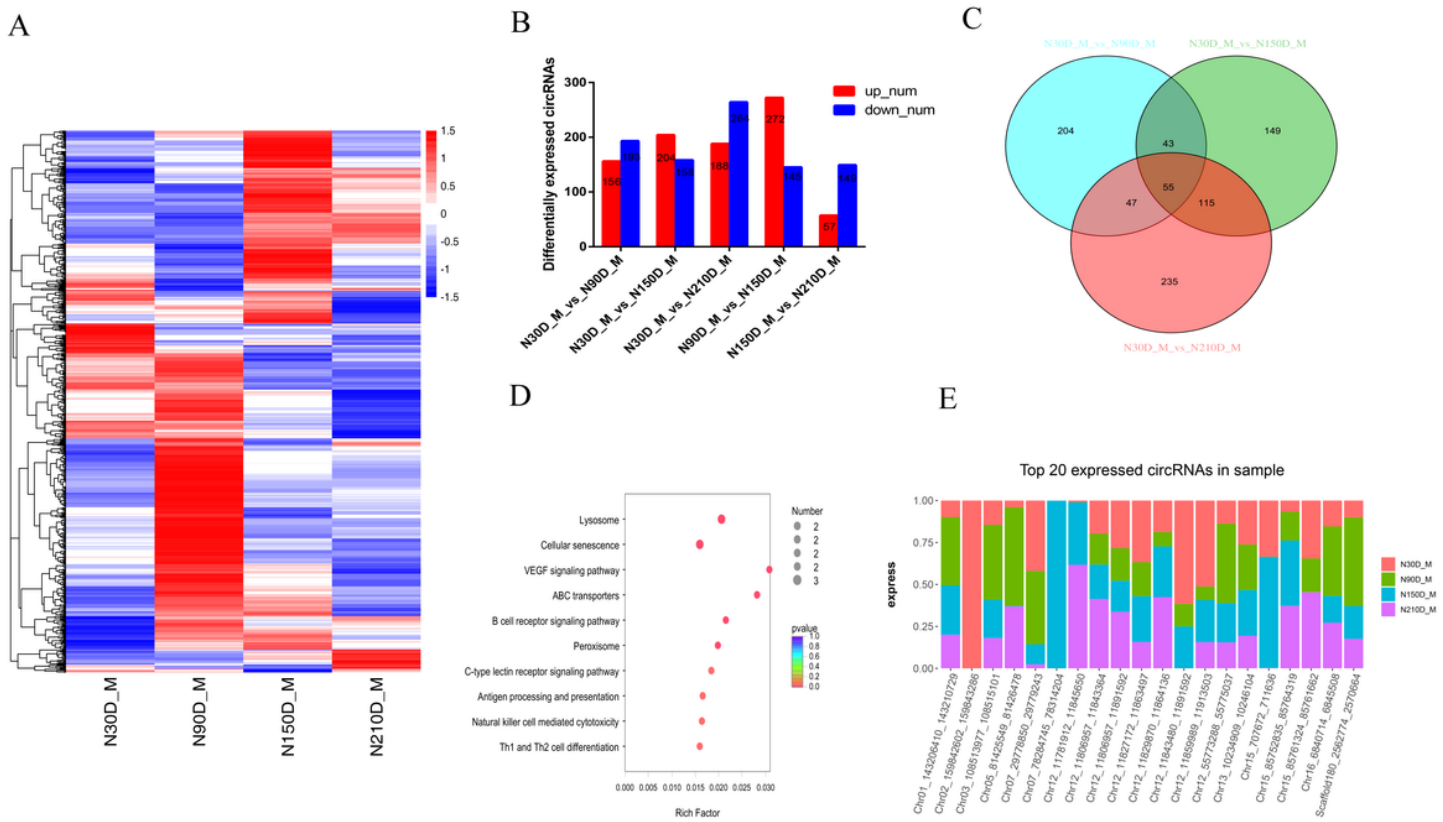

Figure 2

Differentially expressed (DE) circRNAs and their expression modes in skeletal muscle. (A) Heat map of all DE circRNAs among the five compared groups(30d vs 90d, 30d vs 150d, 30d vs 210d, 90d vs 150d, and 150d vs 210d groups). (B) Cluster analysis of differentially expressed circRNAs with the K-means and Hierarchical Clustering method. The x-coordinate is the four development time points, and the y-coordinate is calculated by centered log2-transformed (FPKM+1) circRNAs expression values. Each line represents a circRNA, and the blue line represents the average expression quantity of all circRNAs in the cluster. Each diagram shows only one type of expression pattern.The Numbers inside the brackets represent numbers of circRNAs in each cluster.(C) Number of differentially expressed circRNAs. vs. means versus. (D) The number of common DE circRNAs. (E) Top circRNAs expressed in skeletal muscle.

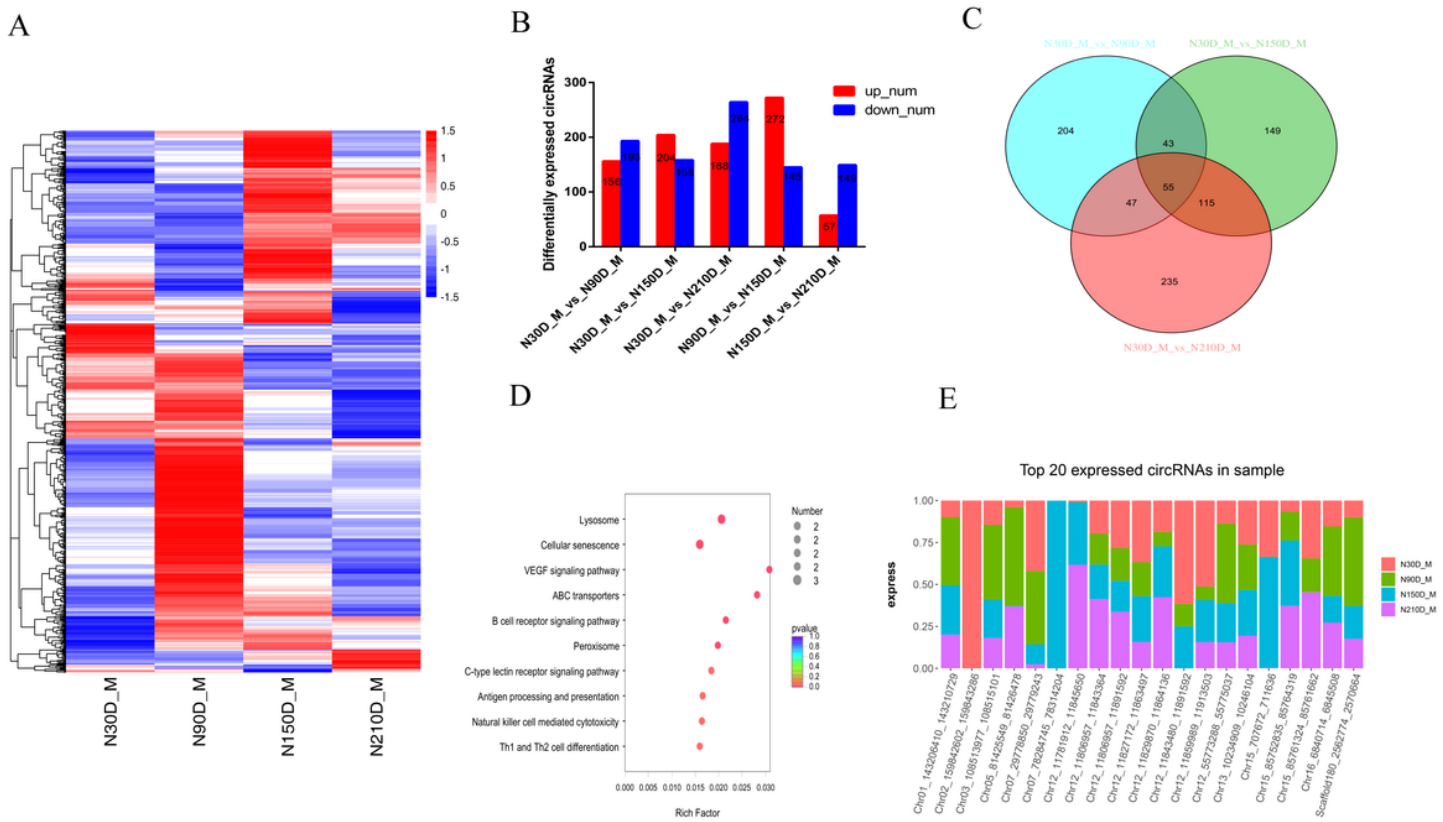

Figure 2

Differentially expressed (DE) circRNAs and their expression modes in skeletal muscle. (A) Heat map of all DE circRNAs among the five compared groups(30d vs 90d, 30d vs 150d, 30d vs 210d, 90d vs 150d, and 150d vs 210d groups). (B) Cluster analysis of differentially expressed circRNAs with the K-means and Hierarchical Clustering method. The x-coordinate is the four development time points, and the y-coordinate is calculated by centered log2-transformed (FPKM+1) circRNAs expression values. Each line represents a circRNA, and the blue line represents the average expression quantity of all circRNAs in the cluster. Each diagram shows only one type of expression pattern.The Numbers inside the brackets represent numbers of circRNAs in each cluster.(C) Number of differentially expressed circRNAs. vs. means versus. (D) The number of common DE circRNAs. (E) Top circRNAs expressed in skeletal muscle.

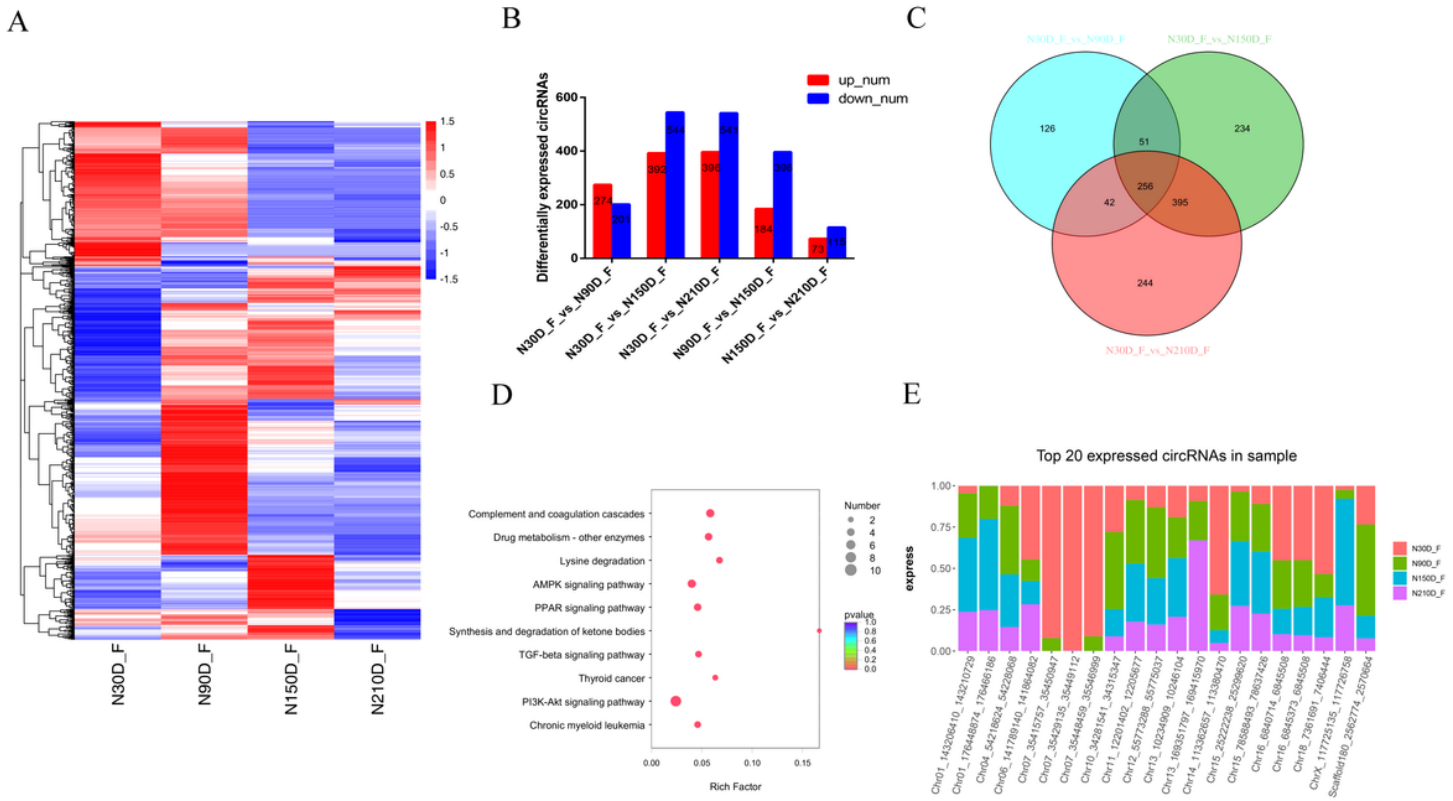

Figure 3

Differentially expressed (DE) circRNAs and their expression modes in fat.(A) Heat map of all DE circRNAs among the five compared groups：30d vs 90d, 30d vs 150d, 30d vs 210d, 90d vs 150d, and 150d vs 210d groups. (B) Cluster analysis of differentially expressed circRNAs with the K-means and Hierarchical Clustering method. (C) Number of differentially expressed circRNAs. vs. means versus. (D) The number of common DE circRNAs. (E) Top circRNAs expressed in fat.

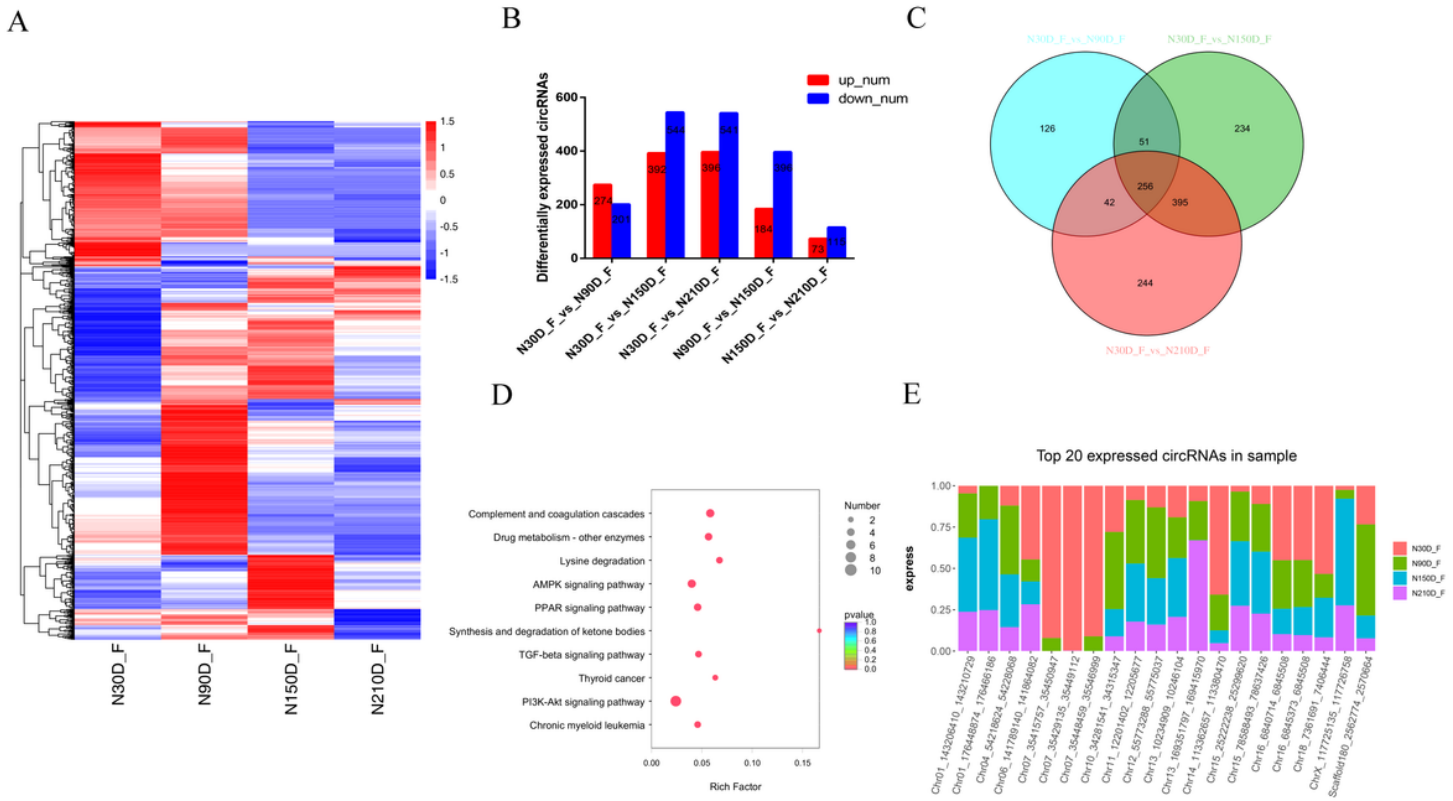

Figure 3

Differentially expressed (DE) circRNAs and their expression modes in fat.(A) Heat map of all DE circRNAs among the five compared groups：30d vs 90d, 30d vs 150d, 30d vs 210d, 90d vs 150d, and 150d vs 210d groups. (B) Cluster analysis of differentially expressed circRNAs with the K-means and Hierarchical Clustering method. (C) Number of differentially expressed circRNAs. vs. means versus. (D) The number of common DE circRNAs. (E) Top circRNAs expressed in fat.

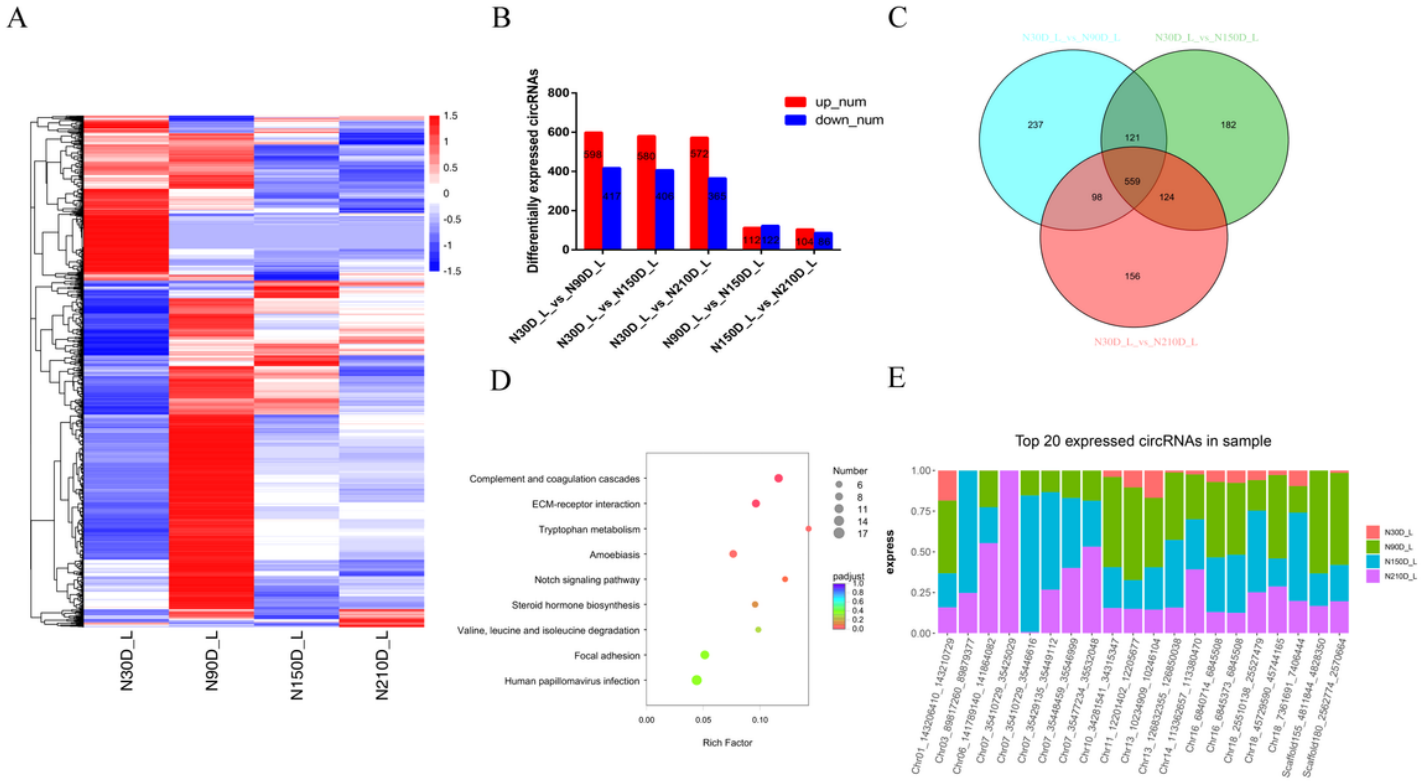

Figure 4

Differentially expressed (DE) circRNAs and their expression modes in liver.(A) Heat map of all DE circRNAs among the five compared groups(30d vs 90d, 30d vs 150d, 30d vs 210d, 90d vs 150d, and 150d vs 210d groups. (B) Cluster analysis of differentially expressed circRNAs with the K-means and Hierarchical Clustering method. (C) Number of differentially expressed circRNAs. vs. means versus. (D) The number of common DE circRNAs. (E) Top circRNAs expressed in liver.

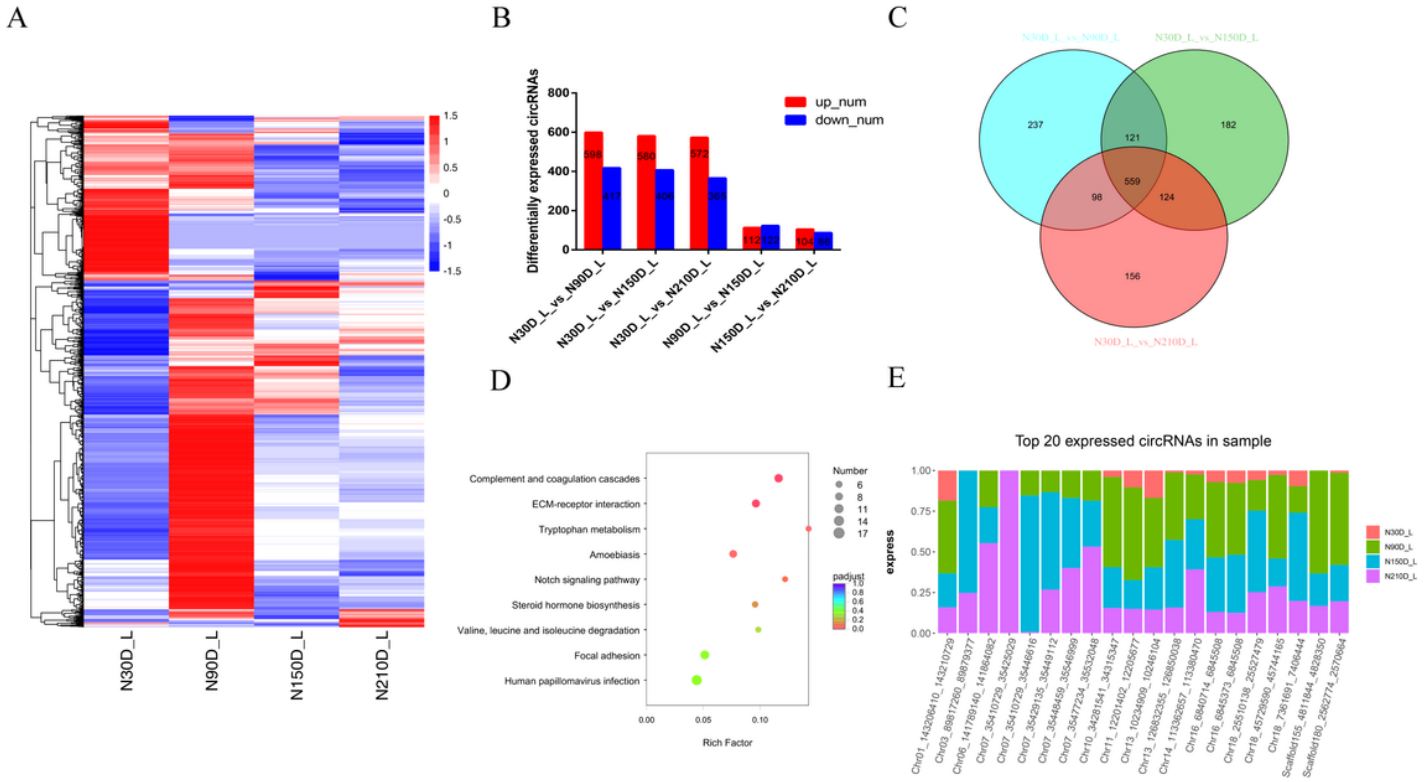

Figure 4

Differentially expressed (DE) circRNAs and their expression modes in liver.(A) Heat map of all DE circRNAs among the five compared groups(30d vs 90d, 30d vs 150d, 30d vs 210d, 90d vs 150d, and 150d vs 210d groups. (B) Cluster analysis of differentially expressed circRNAs with the K-means and Hierarchical Clustering method. (C) Number of differentially expressed circRNAs. vs. means versus. (D) The number of common DE circRNAs. (E) Top circRNAs expressed in liver.

Figure 5

Time-series modules of circRNAs and construction of ceRNA network. Time-series modules of circRNAs in skeletal muscle(A), fat(B),and liver(C). Numbers in the top indicate module number. Numbers in top right corner indicate the statistically significant pvalue value. Numbers in lower left corners indicate numbers of circRNAs in each module. The colored profiles are indicated by different colors (Bonferroni-adjusted P values ≤ 0.05). The P value is sorted from small to large. If the profile is the same color, indicating that these profiles belong to the same cluster. A view of interaction among circRNAs-miRNAs-mRNAs in skeletal muscle(D) , fat(E), and liver(F). Red diamond nodes represent circRNAs，blue circle nodes represent mRNAs; and green arrow nodes represent miRNAs.

Figure 5

Time-series modules of circRNAs and construction of ceRNA network. Time-series modules of circRNAs in skeletal muscle(A), fat(B),and liver(C). Numbers in the top indicate module number. Numbers in top right corner indicate the statistically significant pvalue value. Numbers in lower left corners indicate numbers of circRNAs in each module. The colored profiles are indicated by different colors (Bonferroni-adjusted P values ≤ 0.05). The P value is sorted from small to large. If the profile is the same color, indicating that these profiles belong to the same cluster. A view of interaction among circRNAs-miRNAs-mRNAs in skeletal muscle(D) , fat(E), and liver(F). Red diamond nodes represent circRNAs，blue circle nodes represent mRNAs; and green arrow nodes represent miRNAs.

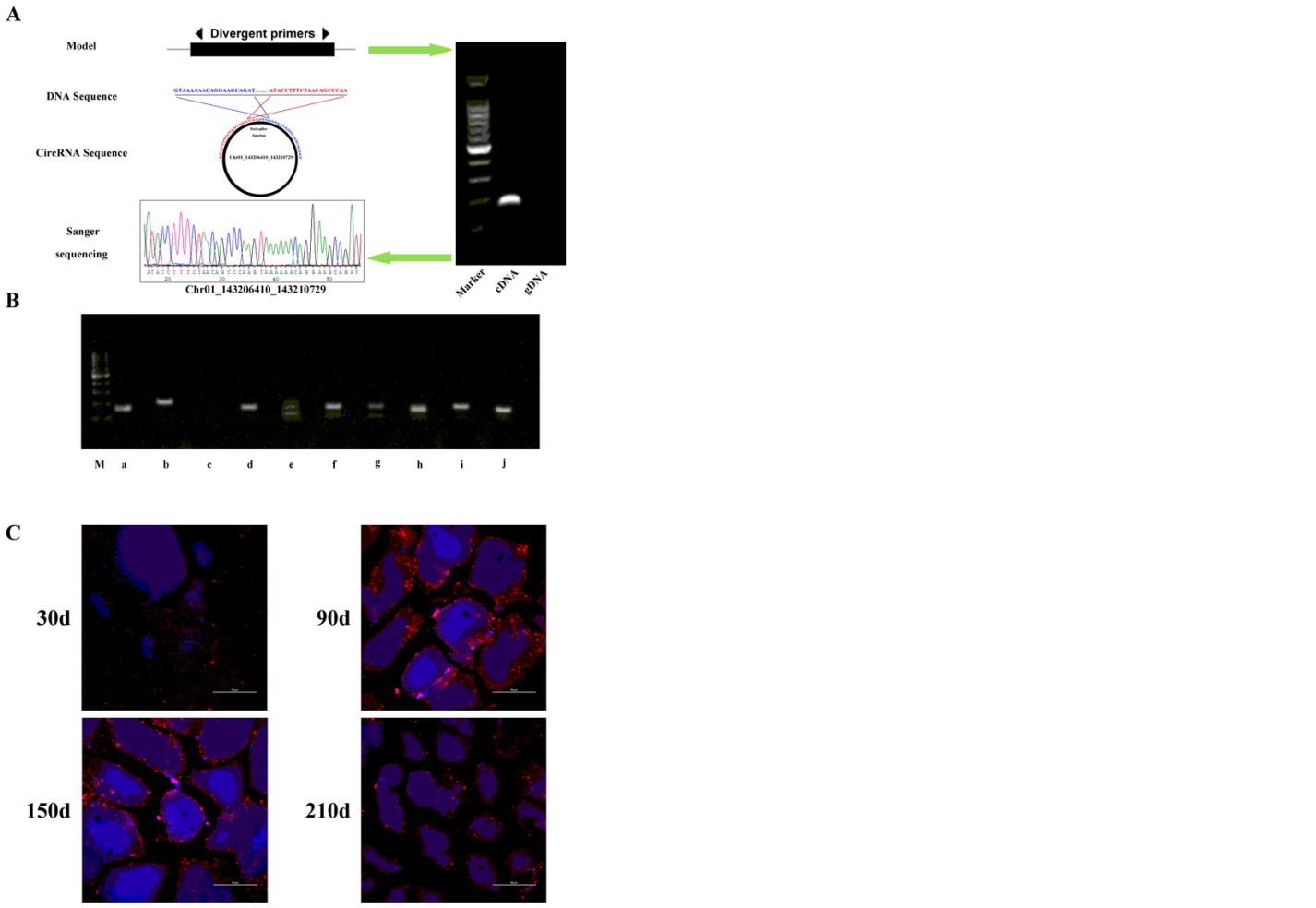

Figure 6

CircRNAs validation by RT-PCR and Sanger sequencing. (A) A representative example circRNA-1687 and (B) nine other circRNAs were showed in the figure. Successfully validated circRNAs: a, Scaffold155_4811844_4828350; b, Scaffold180_2562774_2570664; d, Chr12_55773288_55775037; e, Chr02_159842602_159843286; f, Chr01_176448874_176466186; g, Chr01_143206410_143210729; h, Chr04_99000917_99006790; i, Chr12_27312206_27323763; J, Chr11_12201402_12205677; not successfully validated circRNA: c, Chr18_45729590_45744165; (M, 100bp DNA ladder). Detailed information can be found in Additional Table S20. Black arrows represent the PCR amplification orientation of the divergent primer. (C) Subcellular localization of Chr01_143206410_143210729 in the skeletal muscle at four development time points. Subcellular localization was visualized using panomics probes for high-resolution ISH and DAPI for nuclear localization. Scale bars:50 μm

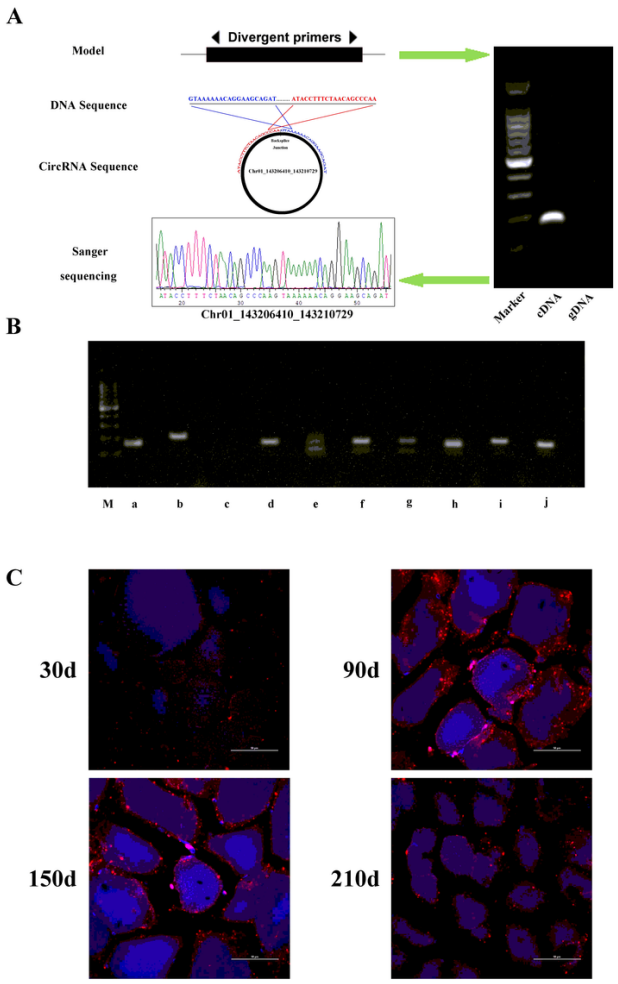

Figure 6

CircRNAs validation by RT-PCR and Sanger sequencing. (A) A representative example circRNA-1687 and (B) nine other circRNAs were showed in the figure. Successfully validated circRNAs: a, Scaffold155_4811844_4828350; b, Scaffold180_2562774_2570664; d, Chr12_55773288_55775037; e, Chr02_159842602_159843286; f, Chr01_176448874_176466186; g, Chr01_143206410_143210729; h, Chr04_99000917_99006790; i, Chr12_27312206_27323763; J, Chr11_12201402_12205677; not successfully validated circRNA: c, Chr18_45729590_45744165; (M, 100bp DNA ladder). Detailed information can be found in Additional Table S20. Black arrows represent the PCR amplification orientation of the divergent primer. (C) Subcellular localization of Chr01_143206410_143210729 in the skeletal muscle at four development time points. Subcellular localization was visualized using panomics probes for high-resolution ISH and DAPI for nuclear localization. Scale bars:50 μm

Supplementary Files

This is a list of supplementary files associated with this preprint. Click to download.

- AdditionalFigure1.tif
- AdditionalFigure1.tif
- AdditionalFigure2.tif
- AdditionalFigure2.tif
- AdditionalTableS1.xlsx
- AdditionalTableS1.xlsx
- AdditionalTableS10.xls
- AdditionalTableS10.xls
- AdditionalTableS11.xls
- AdditionalTableS11.xls
- AdditionalTableS12.xlsx

- AdditionalTableS12.xlsx
- AdditionalTableS13.xlsx
- AdditionalTableS13.xlsx
- AdditionalTableS14.xlsx
- AdditionalTableS14.xlsx
- AdditionalTableS2.xls
- AdditionalTableS2.xls
- AdditionalTableS3.xls
- AdditionalTableS3.xls
- AdditionalTableS4.xls
- AdditionalTableS4.xls
- AdditionalTableS5.xls
- AdditionalTableS5.xls
- AdditionalTableS6.xls
- AdditionalTableS6.xls
- AdditionalTableS7.xls
- AdditionalTableS7.xls
- AdditionalTableS8.xls
- AdditionalTableS8.xls
- AdditionalTableS9.xls
- AdditionalTableS9.xls
- AuthorChecklist.pdf
- AuthorChecklist.pdf